Large Diameter of Palytoxin-induced Na/K Pump Channels and Modulation of Palytoxin Interaction by Na/K Pump Ligands

Pablo Artigas and David C. Gadsby

Laboratory of Cardiac/Membrane Physiology, Rockefeller University, New York, NY 10021

ABSTRACT Palytoxin binds to Na/K pumps to generate nonselective cation channels whose pore likely comprises at least part of the pump's ion translocation pathway. We systematically analyzed palytoxin's interactions with native human Na/K pumps in outside-out patches from HEK293 cells over a broad range of ionic and nucleotide conditions, and with or without cardiotonic steroids. With 5 mM internal (pipette) [MgATP], palytoxin activated the conductance with an apparent affinity that was highest for Na^+-containing (K^+-free) external and internal solutions, lowest for K^+-containing (Na^+-free) external and internal solutions, and intermediate for the mixed external Na^+/internal K^+, and external K^+/internal Na^+ conditions; with Na^+ solutions and MgATP, the mean dwell time of palytoxin on the Na/K pump was about one day. With Na^+ solutions, the apparent affinity for palytoxin action was low after equilibration of patches with nucleotide-free pipette solution. That apparent affinity was increased in two phases as the equilibrating [MgATP] was raised over the submicromolar, and submillimolar, ranges, but was increased by pipette MgAMPPNP in a single phase, over the submillimolar range; the apparent affinity at saturating [MgAMPPNP] remained ~30-fold lower than at saturating [MgATP]. After palytoxin washout, the conductance decay that reflects palytoxin unbinding was accelerated by cardiotonic steroid. When Na/K pumps were preincubated with cardiotonic steroid, subsequent activation of palytoxin-induced conductance was greatly slowed, even after washout of the cardiotonic steroid, but activation could still be accelerated by increasing palytoxin concentration. These results indicate that palytoxin and a cardiotonic steroid can simultaneously occupy the same Na/K pump, each destabilizing the other. The palytoxin-induced channels were permeable to several large organic cations, including N-methyl-d-glucamine$^+$, suggesting that the narrowest section of the pore must be ~7.5 Å wide. Enhanced understanding of palytoxin action now allows its use for examining the structures and mechanisms of the gates that occlude/deocclude transported ions during the normal Na/K pump cycle.

KEY WORDS: Na/K-ATPase • ion-motive pump • ion channel selectivity • outside-out patch recording • toxin binding

INTRODUCTION

The lethal marine toxin, palytoxin, first extracted from the polyps of soft-bodied zoanthids of the genus *Palythoa* (Moore and Scheuer, 1971), is a potentially useful tool for elucidating the molecular reactions by which the Na/K-ATPase stoichiometrically transports Na^+ and K^+ ions in opposite directions across the cell surface membrane. Palytoxin was found to depolarize mammalian cells (e.g., Weidmann, 1977) by causing small-conductance (~10 pS) relatively nonselective cation channels to appear in their surface membranes (e.g., Ikeda et al., 1988; Muramatsu et al., 1988). That the Na/K-ATPase is the target for palytoxin action was initially surmised (Habermann, 1989) largely from antagonism of toxin action by cardiotonic steroids, like ouabain, or by K^+ ions. Two experimental approaches have since confirmed that proposal. The first exploited the absence of endogenous Na/K pumps from yeast and showed that palytoxin could elicit ouabain-sensitive cation flux in yeast expressing both α and β subunits of mammalian Na/K pumps, but not if the yeast expressed either subunit alone (Scheiner-Bobis et al., 1994), nor if the COOH-terminal 44 residues of the α subunit were deleted (Redondo et al., 1996). Moreover, because binding of [^{3}H]-ouabain to intact yeast cells, and its inhibition by palytoxin, established that the truncated Na/K-ATPase was expressed at the cell surface and could interact with either ligand, it seemed that palytoxin somehow opened a cation pathway within, or alongside, intact Na/K pumps. But catalytic integrity was not essential, as palytoxin still elicited ouabain-sensitive cation efflux in yeast expressing mutant Na/K pumps in which the α subunit's phosphate-accepting residue, Asp369, was replaced by Ala (Scheiner-Bobis and Schneider, 1997). The second approach used mammalian $\alpha_3\beta_1$ Na/K pumps synthesized by in vitro translation in a cell-free expression system and then incorporated into a planar phospholipid bilayer, where exposure to palytoxin elicited the characteristic ~10-pS cation channels (Hirsh and Wu, 1997), so dem-

Address correspondence to David C. Gadsby, Laboratory of Cardiac/Membrane Physiology, Rockefeller University, 1230 York Avenue, New York, NY 10021-6399. Fax: (212) 327-7589; email: gadsby@mail.rockefeller.edu

J. Gen. Physiol. © The Rockefeller University Press • 0022-1295/2004/04/357/20 $8.00
Volume 123 April 2004 357–376
http://www.jgp.org/cgi/doi/10.1085/jgp.200308964

onstrating unequivocally that Na/K pumps are the sole requirement for palytoxin action.

More recent results have suggested that the palytoxin-induced pores comprise at least some segment of the ion translocation pathway normally traversed by the pumped Na^+ and K^+ ions. Thus, palytoxin has been shown to render cysteines substituted for several residues in the fifth and sixth putative transmembrane helices (M5 and M6) susceptible to hydrophilic sulfhydryl-specific reagents (Guennoun and Horisberger, 2000, 2002). Functional consequences of mutating some of those residues had already implicated them in cation binding (e.g., Nielsen et al., 1998; Pedersen et al., 1998), and their homologues in the related SERCA-ATPase were found, in high-resolution crystal structures (Toyoshima et al., 2000; Toyoshima and Nomura, 2002), to help coordinate the bound Ca ions. In addition, ion flow through individual palytoxin-induced channels appeared to be controlled by two gates that could be regulated by the Na/K pump's physiological ligands in a way that suggested that gating reflects conformational changes like those underlying the pump's normal ion occlusion/deocclusion partial reactions (Artigas and Gadsby, 2003a,b). Together, these studies suggest that palytoxin interferes with the normally strict coupling between inner and outer sets of gates that control access to cation binding sites within the Na/K pump, and thereby allows the gates to sometimes be open simultaneously. If so, then palytoxin could be a useful tool for characterizing the ion translocation pathway and the structures and mechanisms of the pump's gates.

Before palytoxin can be exploited for such studies, however, its interactions with the Na/K pump must be better understood. Despite much work (for review see Habermann, 1989; Tosteson, 2000), a consistent picture of how palytoxin interacts with the Na/K pump has yet to emerge. This is undoubtedly due to the variety of methods, preparations, and Na/K pump isoforms examined, and the limited range of experimental conditions employed in each study (Tosteson, 2000), as there were early indications that the effects of palytoxin could be influenced by, among other things, extracellular K ions (Ahnert-Hilger et al., 1982; Ishida et al., 1983; Böttinger et al., 1986) or cytoplasmic nucleotides (Chhatwal et al., 1983; Böttinger et al., 1986; Kim et al., 1995). Here we describe an extensive study of palytoxin interactions with native Na/K pumps in HEK293 cells (a human embryonic kidney cell line) and in guinea pig ventricular myocytes. Almost all measurements were made on outside-out excised patches of membrane so that the compositions of solutions at both surfaces could be well controlled. We found that the apparent affinity for the interaction of palytoxin with the same population of Na/K pumps was profoundly influenced by varying the ionic and metabolic conditions. Palytoxin appeared to bind most tightly to phosphorylated Na/K pumps exposed to K^+-free, Na^+-containing external and internal solutions: interestingly, these conditions, combined with physiological cytoplasmic [MgATP], correspond to those found to maximize the open probability of palytoxin-induced channels (Artigas and Gadsby, 2003a). We found that palytoxin and a cardiotonic steroid can both be simultaneously bound to the same Na/K pump, but that each destabilizes the binding of the other. We also present a preliminary characterization of the permeation pathway of the palytoxin-induced channel which suggests that, at its narrowest point, the pore must have a diameter on the order of 7.5 Å.

MATERIALS AND METHODS

Cell Preparation

Human embryonic kidney (HEK293) cells were maintained at 37°C and 5% CO_2 in Dulbecco's modified eagle medium supplemented with 10% fetal bovine serum and penicillin/streptomycin (all from GIBCO-BRL), and then plated on poly-L-lysine–coated glass coverslips in 35-mm Petri dishes for use within 3 d. Guinea pig ventricular myocytes were isolated using collagenase as described (Gadsby and Nakao, 1989), and stored until use (within 24 h) at 4°C in high-K Ca-free solution containing (in mM) 70 K-glutamate, 25 KCl, 20 taurine, 10 KH_2PO_4, 1 $MgCl_2$, 0.5 EGTA, 20 glucose, 10 HEPES (pH = 7.3).

Solutions

For whole-cell and outside-out patch recording, the standard cytoplasmic-side (pipette) solution contained (in mM): 130 L-glutamic acid, 10 HEPES, 10 EGTA, 10 TEACl, 5 MgATP, 1 $MgCl_2$, and 150 NaOH or KOH (or, to measure Na/K pump current, 50 NaOH + 100 CsOH). Tetraethylammonium (TEA) was omitted from the internal solutions containing 160 mM tetrapropylammonium (TPA) or N-methyl-D-glucamine (NMG). The external solution contained (in mM): 140 sulfamic acid, 10 HEPES, 10 HCl, 1 $MgCl_2$, 1 $CaCl_2$, 0.5 $BaCl_2$, and 160 mM of the appropriate monovalent cation (as indicated). For whole-cell measurements of Na/K pump current 1 mM $CdCl_2$ was added to minimize currents through Na^+ and Ca^{2+} channels and the Na/Ca exchanger. MgATP was omitted from nucleotide-free internal solution and intermediate [MgATP] obtained by mixing. When the nucleotides Li_4AMPPNP (5′-adenylylimido-diphosphate) or Na_2ADP (adenosine 5′-diphosphate) replaced MgATP, equimolar $MgCl_2$ was added to keep free [Mg^{2+}] ~1 mM. All internal and external solutions had a pH of 7.4 ± 0.05 and osmolality of 280–305 mOsm/kg.

An aliquot of frozen 100 μM PTX (from *Palythoa toxica*; Calbiochem) aqueous solution was thawed and diluted into external solutions just before each experiment. All PTX-containing solutions also included ~0.002% BSA to reduce PTX binding to non-glass surfaces (Taylor et al., 1991). Strophanthidin was added from a 1-M stock solution in DMSO, and ouabain and dihydroouabain were dissolved in the appropriate external solution at their final concentration.

Electrophysiology

Whole-cell and outside-out membrane patch currents were recorded (Hamill et al., 1981) at 22–25°C using an Axopatch 200B

amplifier, Digidata 1200 A/D board, and pCLAMP 7 software (Axon Instruments, Inc.); currents were filtered at 0.1–2 kHz (Frequency Devices) and sampled at 1–10 kHz. In most experiments data were also continuously recorded on VCR tape via a Neurocorder 384 (Neurodata Instruments Co.). Pipettes were made from thin-walled borosilicate glass (PG52151–4; WPI) using a horizontal (P-2000; Sutter Instruments Co.) or vertical (PP-83; Narishige Scientific Instruments) two-stage puller. Pipette resistances were 0.5–3 MΩ for recording whole-cell currents and 1.6–8 MΩ and 10–30 MΩ for macroscopic and microscopic currents, respectively, in outside-out patches. To minimize liquid junction potentials, a 1-M KCl-agar bridge connected the bath solution to the AgCl pellet reference electrode. Estimated changes (≤3 mV) in junction potentials upon exchanging external solution were used to correct reversal potential shifts before calculating permeability ratios for Cs^+, K^+, and Rb^+.

Solution Exchange System

The flow system comprised up to eight solution lines controlled by computer-driven solenoid valves (General Valve, Parker Instrumentation), only one of which was open at a time, that converged on a miniature glass manifold positioned within ~200 μm of the patch or cell under study. Solution exchange time at that position was estimated from seal current changes after bath solution switches before each experiment; only membrane current responses slower than solution exchange were included in analyses of conductance activation kinetics. Flow lines, manifold, and chamber were often replaced after exposures to high palytoxin concentrations to minimize contamination in subsequent experiments.

Data Analysis

Data were analyzed and fitted with CLAMPFIT (pCLAMP 7) and/or Origin 5.0 (Microcal Corp.) using nonlinear least-squares methods. To determine unitary current amplitudes, all-points histograms were constructed after applying small corrections for linear baseline drifts. The histograms were fitted with sums of Gaussian functions, and the differences between adjacent peaks were plotted against voltage to yield single-channel current-voltage curves.

The permeability of monovalent cation X^+ relative to that for Na^+, P_X/P_{Na}, was calculated from the shift (ΔE_{rev}) in reversal potential of PTX-induced current upon switching from 160 mM external Na^+ to 160 mM external X^+, using the Goldman-Hodgkin-Katz equation, $\Delta E_{rev} = E_{rev,X} - E_{rev,Na} = (RT/F)\ln(P_X/P_{Na})$. This assumes that the composition of the solution at the cytoplasmic surface of the membrane remains unaltered, and that internal and external ions flow independently through the PTX-induced current pathway (e.g., Hille, 1992). In the calculations of permeability ratios of monovalent cations, the contributions of the 1 mM Ca^{2+}, 1 mM Mg^{2+}, and 0.5 Ba^{2+} present in all solutions were ignored because they were found to be only weakly permeant and they were present at a 160-fold smaller concentration than the test ions.

Results are presented as mean ± SEM of indicated number (n) of observations.

RESULTS

Permeation Characteristics of PTX-induced Conductance Pathway

To monitor palytoxin (PTX) interactions with Na/K pumps, we measured changes in the conductance of outside-out patches of membrane excised from HEK293 cells. The prolonged recording in Fig. 1 A shows the large inward shift of membrane current caused by addition of 100 nM PTX, a saturating concentration (Fig. 4, below), to the 160-mM Na^+ solution bathing a patch held at −20 mV with 150 mM Na^+ and

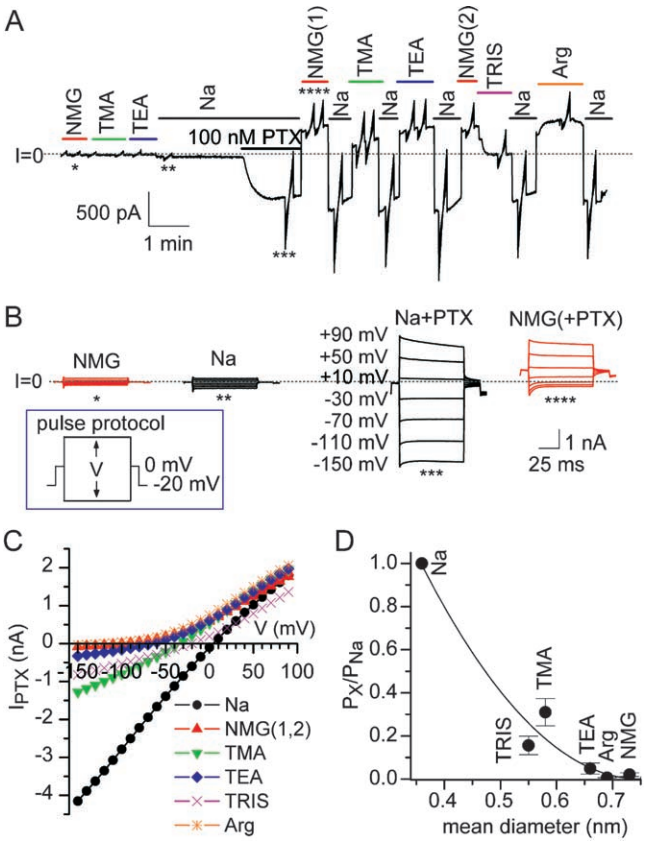

FIGURE 1. Permeation of organic monovalent cations through PTX-induced conductance pathway in outside-out patches from HEK293 cells with internal solution containing 150 mM Na^+ and 5 mM MgATP. (A) Holding current at −20 mV throughout changes in principal external cation (160 mM in each case), and application of 100 nM PTX, indicated by colored and labeled horizontal bars over record; PTX increased inward current with time constant, τ_{inc} = 10 s. The vertical deflections reflect current changes (severely truncated due to the contracted time-scale) due to voltage steps. (B) Superimposed currents elicited (at times marked with asterisks in A) by the 80-ms steps to voltages (V) between −150 and +90 mV (using protocol shown in inset), shown on expanded time scale; for clarity, only every fourth trace is included. (C) PTX-induced current, I_{PTX}, obtained as difference between currents (measured over ~5 ms at end of each step) before and after addition of PTX, plotted against voltage (except that as $Tris^+$ and $arginine^+$ were not tested before PTX in this experiment currents in NMG^+ and TMA^+ before PTX, respectively, were used instead); though less obvious here, in 10 of 11 other patches, outward I_{PTX} at V > +50 mV was 10–30% smaller when the external cation was NMG^+ than when it was Na^+. (D) P_X/P_{Na} estimates plotted against calculated mean diameter of cation X^+; the line is the fit of $P_X/P_{Na} = k(1 - (d_X/d_p))^2$ for ions of diameter d_X traversing a water-filled pore of diameter d_p = 7.5 Å, with proportionality constant k = 5.6 that incorporates the diameter of the hydrated Na^+ ion (e.g., Dwyer et al., 1980).

5 mM MgATP in the intracellular (pipette) solution. The inward current represents inflow of Na^+ ions, under the influence of the ~20-mV inward driving force, through the thousands of opened channels resulting from PTX action on every Na/K pump in the membrane patch; maximal PTX-induced current in 12 patches under these conditions was 930 ± 170 pA, indicating an average of ~7,000 pump channels per patch, given their open probability of ~0.9 and single-channel conductance of ~7.5 pS (Fig. 3, below). The time course of current increase was approximately exponential under these conditions, with time constant τ_{inc} = 9 ± 2 s (n = 7). Despite washout of all unbound toxin a few seconds later, the current returned to practically the same level during each of the subsequent five reexposures to Na-containing solution, suggesting that PTX remained bound for many minutes, implying a low rate of toxin unbinding (see also Fig. 4 A, below).

We examined selectivity of PTX-induced channels by measuring near steady-state current-voltage relationships in the presence of various external cations (with constant 150 mM Na^+ in the pipette), both before and after opening the channels with PTX. The ramp-like current deflections during the exposure to PTX (Fig. 1 A, ***) indicate large changes in current elicited by 80-ms steps to membrane potentials from −150 to +90 mV, reflecting the increased conductance of the membrane caused by PTX. The barely discernible current deflections in Na^+ solution (Fig. 1 A, **) before addition of PTX confirm that membrane conductance was initially low. Examples of these current changes are shown on a greatly expanded time-scale in Fig. 1 B. Current levels near the end of every step before PTX were subtracted from those after exposure to PTX to yield the PTX-induced currents (I_{PTX}) shown in the current-voltage plot labeled "Na" (Fig. 1 C, ●). The PTX-induced current reversed sign near 0 mV, as expected for current carried by the principal cation, Na^+, present at roughly the same concentration on both sides of the membrane.

Switches between the Na^+ external solution and solutions containing instead 160 mM NMG^+, TMA^+, or TEA^+ before PTX caused only negligibly small changes in holding current, and current deflections in response to the voltage steps were also small (e.g., NMG^+, Fig. 1 B). But, after PTX exposure, the voltage-elicited current changes became considerably larger in all these solutions, and replacing Na^+ by any of these cations (or by $Tris^+$, or $arginine^+$) caused large outward shifts of holding current (Fig. 1 A), indicating that they were all less permeant than Na^+ through the PTX-induced channels. PTX-induced current-voltage plots show that for each of these organic cations the outward current shift reflected a negative shift of the reversal potential (e.g., from +5 mV in Na^+ to −90 mV in NMG^+, Fig. 1 C). On the assumption that external solution exchange was quick enough to allow internal [Na^+] to remain constant, the observed shift in reversal potential for each cation (relative to Na^+) was used to calculate the ratio of permeability coefficients, P_X/P_{Na} (see MATERIALS AND METHODS): e.g., P_{NMG}/P_{Na} averaged 0.021 ± 0.002 (n = 11). Plotting these permeability ratios against the mean diameters (geometric mean of three dimensions of the smallest box to contain a space-filling model) of the cations (dehydrated for the organic cations, hydrated for Na^+; Robinson and Stokes, 1965; Villarroel et al., 1995) suggests that permeability falls to near zero when the mean diameter of the cation is ~7 Å (Fig. 1 D). Indeed, an estimate of 7.5 Å for the diameter of the narrowest part of the PTX-induced channel pore was obtained by fitting to the data (Fig. 1 D, curve) a simplified model (e.g., Dwyer et al., 1980) in which the cross-sectional area available to permeating ions determines the permeability of a rigid cylindrical water-filled pore.

To verify that the small inward PTX-induced currents at very negative potentials in external NMG^+ solution truly reflected inflow of NMG^+ ions, and not of Na^+ ions that had exited the pipette through the PTX-opened channels and accumulated in some poorly-stirred external layer, we repeated the measurements after replacing all Na^+ in the pipette solution with large monovalent cations (Fig. 2). With 160 mM pipette NMG^+ (and 5 mM MgATP, as usual), addition of 100 nM PTX to the 160-mM NMG^+-containing external solution caused an inward shift of membrane current (at the −20-mV holding potential), with a time course (τ_{inc} = 15 ± 6 s, n = 6) comparable to that seen with all-Na^+ solutions, but with an amplitude smaller by one or two orders of magnitude (Fig. 2 A, left). As found with Na^+-containing external solution, despite washout of unbound toxin, the inward current level during the final exposure to NMG^+ solution was unchanged (Fig. 2 A, left), suggesting that PTX also dissociated slowly under these experimental conditions. In addition, the voltage-induced current deflections as well as the shifts of membrane current caused by switching between external solutions containing 160 mM NMG^+ or 160 mM TPA^+, or by diluting the NMG^+ solution ~10-fold (15 mM NMG^+) with isotonic sucrose, were all much larger after PTX exposure than before. The corresponding PTX-induced current-voltage plots (Fig. 2 A, right), all obtained with 160 mM internal NMG^+, confirm that NMG^+ ions do indeed permeate PTX-induced channels in both directions. Moreover, the negative reversal potential shift due to the 10-fold reduction in [NMG^+] averaged −60 ± 5 mV (n = 3), close to the −59-mV estimated shift in equilibrium potential for NMG^+ ions. This suggests that the simultaneous 10-fold reduction in [$sulfamate^-$] was of little consequence, and hence

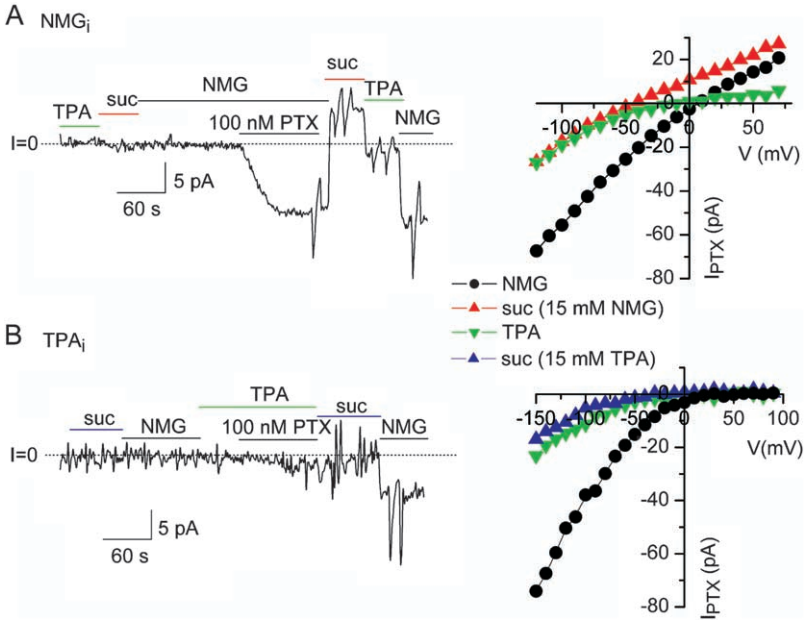

FIGURE 2. NMG^+, but not TPA^+, ions permeate PTX-induced pathway. (A, left) Current at −20 mV in outside-out HEK293 cell patch with internal solution containing 160 mM NMG^+ and 5 mM MgATP, and changes in external solutions indicated by bars over record. 100 nM PTX increased inward current (τ_{inc} = 18 s) in NMG^+ solution, but current was unchanged in TPA^+ and was outward after an ~10-fold dilution with sucrose (suc, 15 mM NMG^+). (Right) I_{PTX}-V plots determined by subtraction (as in Fig. 1) of currents during 80-ms voltage steps applied (during deflections in record at left) in each solution before and after PTX application; note that external TPA^+ reduced outward I_{PTX} carried by NMG^+. (B, left) As in A, but internal solution contained 160 mM TPA^+; 100 nM PTX did not increase current at −20 mV in TPA^+ external solution but did increase inward current in NMG^+. (Right) Resulting I_{PTX}-V plots (from experiment at left) showing inward current carried by NMG^+ but absence of inward and outward TPA^+ current.

that the PTX-induced channels are essentially impermeable to these large anions.

In contrast, only very small PTX-induced currents were seen in the external solution containing 160 mM TPA^+ (Fig. 2 A, right). To examine this further, we used 160 mM TPA^+ internal solution and repeated the experiment (Fig. 2 B). Under these conditions, little or no PTX-induced current was discernible when 160 mM TPA^+ was present also in the external solution, and there was no response to an ~10-fold dilution of the external TPA^+ solution with isotonic sucrose solution (Fig. 2 B). However, after washout of unbound PTX, a switch to NMG^+ external solution elicited a rapid inward current shift and revealed a PTX-induced inward current-voltage relationship (Fig. 2 B, right) comparable to that observed under the conditions of Fig. 2 A. As the PTX had already been washed out, the fact that the inward current was activated more rapidly in Fig. 2 B than in Fig. 2 A suggests that PTX had in fact bound to the Na/K pumps in TPA^+ external solution, and transformed them into ion channels, but that TPA^+ was too large a cation to permeate them. This conclusion is supported by the evident inability of the 160 mM internal TPA^+ to carry any outward PTX-induced current at large positive membrane potentials (even during exposure to NMG^+ external solution, when substantial inward currents were seen at negative potentials; Fig. 2 B, right). Indeed, TPA^+ appeared to exert some blocking effect as outward currents carried by NMG^+ were reduced, reversibly, during exposure to TPA^+ external solution (Fig. 2 A). These results establish that the ion pathway underlying the PTX-induced conductance is wide enough to allow permeation of NMG^+ (mean diameter, 7.3 Å), but narrow enough to preclude permeation of TPA^+ (mean diameter, 8–9 Å).

Experiments like that in Fig. 1 (using the same Na^+-containing internal solution) yielded permeability ratios, relative to Na^+, for other alkali metal cations: P_K/P_{Na} = 1.13 ± 0.02 (n = 6), P_{Cs}/P_{Na} = 1.01 ± 0.01 (n = 3), and P_{Rb}/P_{Na} = 1.11 ± 0.02 (n = 2) (Artigas and Gadsby, 2003b). These ratios confirm earlier reports that the PTX-induced conductance pathway selects poorly among monovalent inorganic cations (e.g., Ikeda et al., 1988; Muramatsu et al., 1988; Tosteson et al., 1991; for review see Tosteson, 2000). In agreement with findings on neuroblastoma cells (Rouzaire-Dubois and Dubois, 1990) and red blood cells (Tosteson et al., 1991), we also found the divalent cations Ca^{2+}, Ba^{2+}, and Mg^{2+} to be weakly (≤NMG^+), but demonstrably, permeant through PTX-induced channels: e.g., holding current of HEK293 cells (held at −20 mV, with NMG^+ internal solution) shifted inward on addition of 100 nM PTX to isotonic Ca^{2+} solutions devoid of monovalent cations (not depicted). The low permeability explains previous failure to observe PTX-induced Ca^{2+} currents in single-channel recordings (Ikeda et al., 1988).

Single-channel Characteristics of PTX-induced Channels

To confirm that the large PTX-induced currents in HEK293 cells (Fig. 1) and cardiac myocytes (Fig. 10, below) flow through channels with characteristics like those previously reported (e.g., Muramatsu et al., 1988; Ikeda et al., 1988; Kim et al., 1995), we recorded currents in individual PTX-induced channels. The high density of Na/K pumps (>1,000 μm^{-2}) in both cell types, and their high apparent affinity for PTX, make

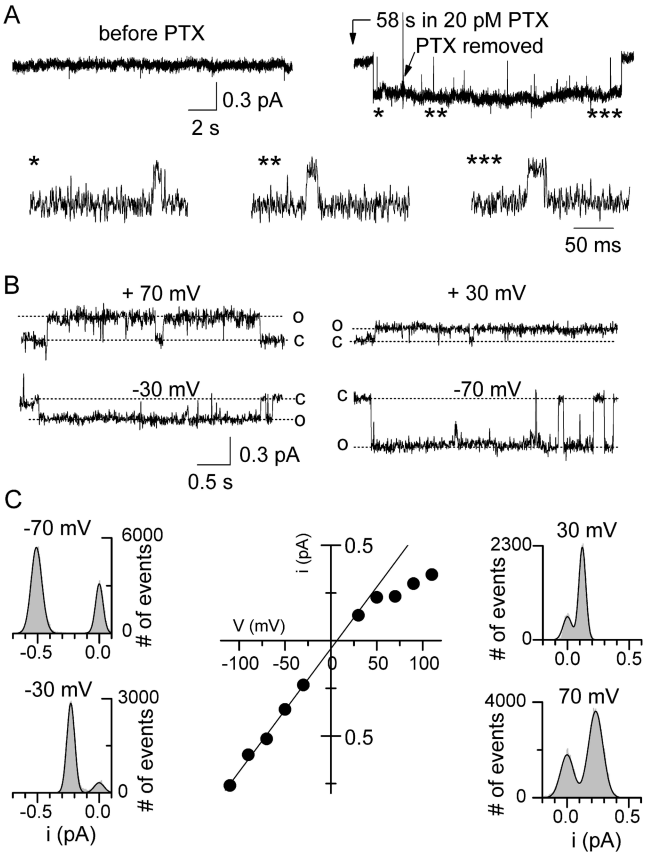

FIGURE 3. Small-conductance channels underlie PTX-induced current. (A, top left) Absence of channel activity in an outside-out ventricular-myocyte patch held at −40 mV, with external and internal Na^+ solutions and 5 mM internal MgATP, before PTX application. (Right) A single PTX-induced channel opened ~1 min after application of 20 pM PTX and its activity, characterized by long open bursts with brief closures (e.g., asterisks), continued long after PTX washout. (Bottom) Examples of brief intraburst closures (asterisks, above) shown on expanded time scale; no baseline subtraction was used. (B) Records of current through same channel as in A at indicated voltages, several min after PTX withdrawal; channel closed (c) and open (o) current levels are marked (baseline was corrected for a linear slope). (C, left and right) All-point histograms of baseline-corrected records ≥20 s long (hence not representative of open probability), fitted with sums of two Gaussians. (Center) Single-channel current, i (differences between Gaussian peaks), plotted against V; linear fit to data at negative V gave channel conductance of 7 pS.

recording single-channel currents in inside-out patches extremely difficult. So we used outside-out patches with 150 mM Na^+ and 5 mM MgATP in the pipette, and added 20 pM PTX to the 160-mM Na^+ external solution until a channel appeared (after ~1 min in the case of the myocyte patch in Fig. 3 A), whereupon unbound PTX was promptly washed away. Because PTX unbinds slowly under these conditions (e.g., Figs. 1 and 4), the channel continued gating for many minutes, with a high open probability (P_o = 0.93 ± 0.02, n = 3; Artigas and Gadsby, 2003a), due to prolonged open bursts that were interrupted by brief intraburst closures (e.g., Fig. 3 A, asterisks) and that were separated by somewhat longer interburst shut times. Recordings at different membrane potentials (e.g., Fig. 3 B) yielded single-channel current-voltage plots (e.g., Fig. 3 C) displaying weak inward rectification. Linear fits over the negative voltage range (e.g., line, Fig. 3 C) gave single-channel conductances that averaged 7.1 ± 0.8 pS (n = 4) for patches from myocytes, and 7.7 ± 0.3 pS (n = 4) for patches from HEK293 cells (two with 5 mM, and two with <1 μM MgATP in the pipette).

Consistent with the macroscopic permeability measurements, the conductance of single PTX-induced channels (Na^+ internal solution with or without ATP) with Cs^+ as the external cation was 1.15 ± 0.02 (n = 2) -fold, and with external K^+ was 1.22 ± 0.15 (n = 4) -fold, that with Na^+ internal and external solutions.

Interaction of PTX with Na/K Pumps

To establish a basis for understanding the variability in published apparent affinities for PTX interaction with the Na/K pump (for review see Tosteson, 2000), we systematically examined those interactions using the same preparation, outside-out patches excised from HEK293 cells, but over a wide range of ionic and nucleotide conditions.

Interactions in Symmetrical (Internal and External) High [Na^+] or High [K^+] Solutions

We began with 5 mM MgATP and 150 mM Na^+ in the pipette (cytoplasmic-side solution), and 160 mM external Na^+ solution. Because the dissociation rate of PTX is extremely low under those conditions (e.g., Fig. 1 A), we attempted to determine cumulative [PTX]-response curves by applying progressively increasing concentrations of PTX and waiting for the resulting current increment to approach steady-state. At the lowest concentrations tested, 8 and 10 pM PTX, the slow current increase necessitated exposures lasting up to 45 min (Fig. 4 A). For each [PTX], the time course of the increase in current could be reasonably approximated by a single exponential function (e.g., Fig. 4 A, dotted fit lines) from which the rates could be estimated and steady-state current increments extrapolated; the fits at 8 and 10 pM in Fig. 4 A yielded τ_{inc} = 1,971 s and 1,442 s, respectively. The switch to 1 nM PTX produced a much faster current increase (τ_{inc} = 210 s; Fig. 4 A) to a near maximal level, as there was little further response to 10 or 100 nM PTX; in other patches, these higher concentrations were applied alone to obtain corresponding τ_{inc} estimates. After withdrawal of the toxin, the PTX-induced current decayed extremely slowly (note the 2.5-fold contraction of time scale in Fig. 4 A): assuming eventual return to the original current baseline, an exponential fit (fit line largely obscured by data, Fig. 4 A)

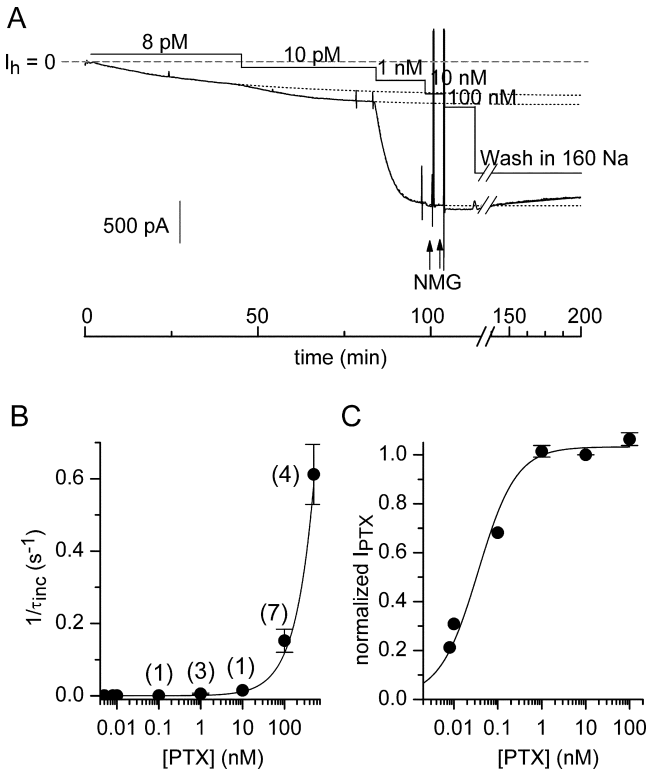

FIGURE 4. Dependence on [PTX] of I_{PTX} activation rate and magnitude in outside-out HEK293 cell patches, at −20 mV, with external and internal Na^+ solutions and 5 mM internal MgATP. (A) The inward current increase in response to each increment in [PTX] was approximately exponential (dotted fit lines), with τ_{inc} = 1,971 s at 8 pM, 1,442 s at 10 pM, and 210 s at 1 nM PTX; dashed line marks zero holding current, I_h. Note contraction of slow time scale after PTX washout; exponential fit (line obscured by data points) to I_{PTX} decay (to $I_h = 0$) gave $\tau_{dec} = 10^5$ s. Brief switches to external solution with all Na^+ replaced by NMG^+ (arrows labeled NMG) verified absence of seal breakdown, as the reversal potential of PTX-induced current with external NMG^+ and internal Na^+ is approximately −90 mV (e.g., Fig. 1), whereas that for the conductance of a broken seal is not far from 0 mV. (B) Mean (±SEM) rate of activation of I_{PTX} ($1/\tau_{inc}$) from exponential fits in 1–7 experiments as in A (one experiment each at 5, 8, and 10 pM), plotted against log [PTX]. The line shows a least-squares linear fit of $1/\tau_{inc} = k_{on}[PTX] + k^*_{off}$ to the data (but with k^*_{off} fixed at 0 s^{-1}), yielding k_{on} = 1.4 (±0.1) × 10^6 $M^{-1}s^{-1}$. (C) Estimated (from the exponential fits as in A) steady-state amplitude of I_{PTX} (normalized to its level at 10 nM PTX) plotted against log [PTX]. The line shows a least-squares fit of a Michaelis function to the data from 4 patches, yielding $K_{0.5PTX}$ = 33 ± 7 pM.

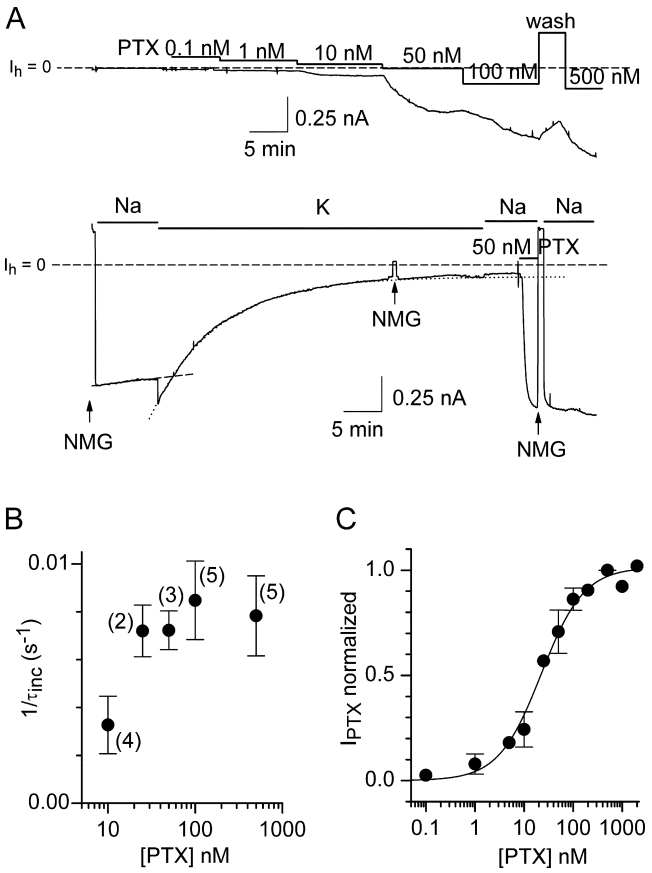

FIGURE 5. Influence of K^+ ions on interactions between PTX and Na/K pumps. (A) Activation of I_{PTX} at −20 mV by incremental increases in [PTX] in an outside-out HEK293 cell patch with 160-mM external K^+ and 150-mM internal K^+ solution with 5 mM MgATP. I_{PTX} requires [PTX] ≥ 1 nM and the activation rate (from exponential fits; omitted for clarity) saturated at $1/\tau_{inc}$ ~0.01 s^{-1} at high [PTX]. Lower record is continuation (~2.5 min omitted) of upper experiment after PTX washout and brief switches to Na^+ and then NMG^+ external solution. Current decay was slow in Na^+ external solution (τ_{dec} = 6,000 s; dashed exponential fit line), but rapid in K^+ external solution (τ_{dec} = 500 s; dotted exponential fit line). After complete decay of I_{PTX}, note that reactivation of I_{PTX} by 50 nM PTX was faster in Na^+ external solution than it had been in K^+ external solution. (B) Means (±SEM) of *n* (in parentheses) measurements of I_{PTX} activation rate, $1/\tau_{inc}$, from exponential fits, plotted against log [PTX]. (C) Dependence on log [PTX] of steady-state amplitude of I_{PTX} (estimated from exponential fits) normalized to its level at 500 nM PTX. The line shows a least-squares fit of a Michaelis function to the data from seven patches, yielding $K_{0.5PTX}$ = 22 ± 2 nM.

suggests τ_{dec} ~10^5 s (fits to somewhat shorter current decays after PTX washout in two other patches gave estimates for τ_{dec} of 2 × 10^4 s and 5 × 10^4 s).

Up to 500 nM PTX, the conductance activation rate $1/\tau_{inc}$ increased linearly with [PTX] (Fig. 4 B, fit line), consistent with the relationship $1/\tau_{inc} = k_{on}[PTX] + k^*_{off}$, (in which $k^*_{off} = 1/\tau_{dec}$ is negligibly small, as observed), which suggests that PTX binding is the rate-limiting step for channel opening under these conditions: the fit gave k_{on} = 1.4 ± 0.1 × 10^6 $M^{-1}s^{-1}$. The [PTX] dependence of the steady-state level of PTX-induced current, I_{PTX}, extrapolated for low [PTX] and normalized to the current at 10 nM, was reasonably well described by a Michaelis-Menten function (Fig. 4 C, fit line), with $K_{0.5PTX}$ = 33 ± 7 pM.

For comparison, we repeated these measurements after replacing all Na^+ with K^+; i.e., we used 160 mM external K^+, and 150 mM K^+ and 5 mM MgATP in the pi-

pette. Two major consequences were immediately evident (Fig. 5 A): activation of measurable current required ~1,000-fold higher concentrations of PTX, and the rate of conductance activation remained low even at the highest PTX concentrations. That this slower activation is attributable to the substitution of extracellular K^+ for Na^+ ions is directly confirmed by the much faster activation of PTX-induced current when 50 nM PTX was applied later to the same patch after switching to Na^+-containing external solution (Fig. 5 A, continuation of recording in lower panel).

The fact that washout of PTX had led to the recovery of baseline conductance, allowing that subsequent reapplication of PTX, points to another distinction between extracellular Na^+ and K^+ ions. Namely, after withdrawal of PTX (after equilibration with 500 nM PTX) the current decay was extremely slow in the presence of external Na^+ (τ_{dec} ~6,000 s; Fig. 5 A, dashed fit line) but was accelerated >10-fold upon switching to external K^+ (τ_{dec} ~500 s, dotted fit line; mean $1/\tau_{dec} = 3 \pm 1 \times 10^{-3}$ s^{-1}, $n = 4$). This relatively rapid current return to near the starting level, and full reinstatement of maximal PTX-induced current on reapplication of PTX, confirms that the current decay reflected unbinding of PTX. The sudden increase in current upon switching from Na^+ to K^+ solution is accounted for by the ~15% higher permeability of PTX-induced channels for K^+ than for Na^+ ions described above.

The saturating dependence of the activation rate on [PTX] (Fig. 5 B) implies that a slow step, distinct from PTX binding to the pump, rate-limits activation of the conductance at high [PTX] in K^+ solutions. The influence of [PTX] on steady-state current (normalized to that at 500 nM) was again reasonably approximated by Michaelis kinetics with $K_{0.5PTX} = 22 \pm 2$ nM (Fig. 5 C). This ~1,000-fold lower apparent affinity for PTX in all-K^+ solutions than found with all-Na^+ solutions seems only partly attributable to the observed ~100-fold increase in the rate of current decline that likely reflects PTX unbinding (compare Figs. 4 A and 5 A) in all-K^+ solutions.

External K^+ Is Responsible for the Low Rate of Conductance Activation at Saturating [PTX]

To further examine which of the two ions, on which side of the membrane, was responsible for these differences, we repeated the PTX concentration-response measurements after changing the ion on only one side of the membrane at a time, i.e., with Na^+ outside and K^+ inside (Na_o/K_i; Fig. 6, A and B), or with K^+ outside and Na^+ inside (K_o/Na_i; Fig. 6, C and D). When PTX was applied in 160 mM external Na^+ solution with 150 mM K^+ and 5 mM MgATP in the internal solution, the activation rate of the PTX-induced current showed no sign of saturation up to 100 nM [PTX] (Fig. 6 A) and the linear fit to $1/\tau_{inc} = k_{on}[PTX] + k^*_{off}$ gave $k_{on} = 8.3 \pm 0.3 \times 10^5$ $M^{-1}s^{-1}$, using the single estimate of k^*_{off} ($= 1/\tau_{dec} = 10^{-4}$ s^{-1}) obtained directly from current decay after PTX washout; this k_{on} is comparable to the value we obtained with all-Na^+ solutions. However, the apparent affinity for activation of steady-state current by PTX in this mixed Na_o/K_i condition, which yielded $K_{0.5PTX} = 0.27 \pm 0.07$ nM (Fig. 6 B), was intermediate between that found in all-K^+ or all-Na^+ solutions (10-fold lower affinity than in all-Na^+).

In the complementary biionic condition, with 160 mM external K^+ solution and with 150 mM Na^+ and 5 mM MgATP in the internal solution, the rate of activation of the PTX-induced current remained low as [PTX] was increased and it saturated at high [PTX] (e.g., ≥50 nM; Fig. 6 C), similar to our findings with all-K^+ solutions. The current decay rate, related to PTX

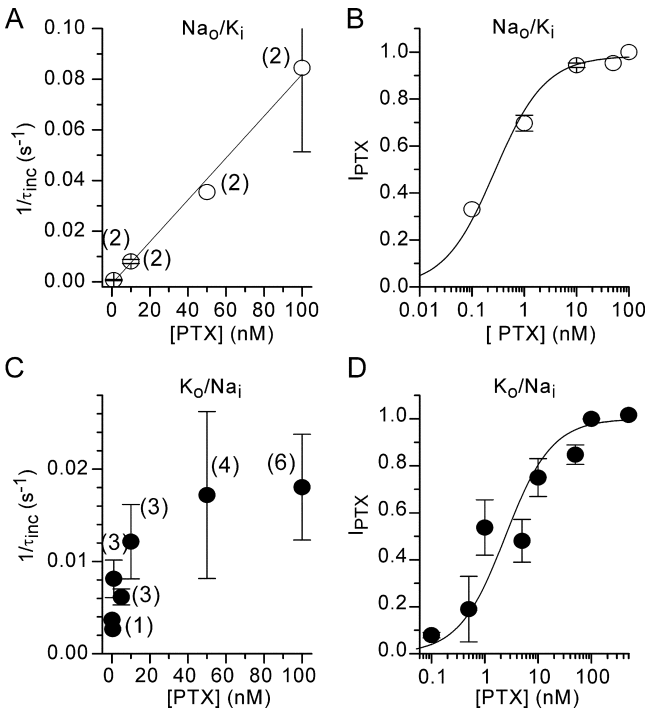

FIGURE 6. Dependence of I_{PTX} activation rate and magnitude on [PTX] under mixed Na^+ and K^+ (biionic) conditions, from experiments on outside-out HEK293 cell patches as in Figs. 4 and 5. (A) Mean (±SEM, of n measurements) $1/\tau_{inc}$ plotted against [PTX]. (B) Estimated steady amplitude (normalized to that at 100 nM PTX), of I_{PTX}, from two patches plotted against log [PTX], determined with 160 mM external Na^+ and 150 mM internal K^+ solution with 5 mM MgATP. The line in A shows a fit to $1/\tau_{inc} = k_{on}[PTX] + k^*_{off}$ (with k^*_{off} fixed at the observed 10^{-4} s^{-1}), yielding $k_{on} = 8.3 \pm 0.3 \times 10^5$ $M^{-1}s^{-1}$. The Michaelis fit in B gave $K_{0.5PTX} = 0.27 \pm 0.07$ nM. (C and D) Corresponding $1/\tau_{inc}$ vs. [PTX], and estimated steady I_{PTX} vs. log [PTX], respectively, from seven patches with 160 mM external K^+ and 150 mM internal Na^+ solution with 5 mM MgATP. The large error bars in C reflect patch-to-patch variation, as saturation of $1/\tau_{inc}$ was a consistent finding in individual patches: thus $1/\tau_{inc}(50\text{ nM})/1/\tau_{inc}(10\text{ nM}) = 1.5 \pm 0.4$ ($n = 3$). The Michaelis fit in D gave $K_{0.5PTX} = 2.4 \pm 0.8$ nM.

unbinding, in this mixed K_o/Na_i condition was $1/\tau_{dec} = 9 \pm 3 \times 10^{-4}\ s^{-1}$ ($n = 7$), some threefold slower than with all-K^+ but ~30-fold faster than with all-Na^+ solutions. Similarly, PTX increased steady-state current in the mixed K_o/Na_i condition with an apparent affinity ($K_{0.5PTX} = 2.4 \pm 0.8$ nM; Fig. 6 D) intermediate between those found in all-K^+ or all-Na^+ solutions (100-fold lower affinity than in all-Na^+). The faster (compared with external Na^+) current decay after PTX washout elicited by external K^+ was also observed with external Cs^+, Rb^+, or Tl^+ solutions but not with external solutions of the organic cations NMG^+ or TMA^+, and qualitatively similar results were obtained whether the internal solution contained Na^+ or K^+.

Evidently, regardless of whether the internal solution contained K^+ or Na^+, the presence of 160 mM external K^+ severely limited the rate of activation of PTX-induced current at maximal [PTX] (Figs. 5 B and 6 C), and (compared with external Na^+) increased $K_{0.5PTX}$ ~100-fold (Figs. 5 C and 6 D vs. Figs. 6 B and 4 C). This uniformity of external cation effects, together with the consistent ~10-fold increase of $K_{0.5PTX}$ caused by replacing internal Na^+ with K^+, regardless of external cation (Figs. 4 C and 6 D vs. Figs. 6 B and 5 C), mitigates against major distortion of these results by intrapipette accumulation (estimated to be ≤8 mM; see Kang et al., 2003) of ions flowing through opened channels at the −20-mV holding potential. An important mechanistic question is whether this influence of extracellular K^+ is mediated by K^+ ions binding to their transport sites in the Na/K pump. If so, the rate of current activation at high [PTX] may be expected to display a dependence on external [K^+] comparable to that found for K^+ transport by the Na/K pump. Indeed, with internal solution containing 150 mM Na^+ and 5 mM MgATP, current activation by 100 nM PTX was slowed by external [K^+] (replacing extracellular Na^+; Fig. 7 A), with $K_{0.5K} = 2.4 \pm 1.2$ mM (Fig. 7 B), near values for Na/K pump current stimulation by external K^+, in the presence of external Na^+, in HEK293 cells (1.5 mM; Kocksämper et al., 1997) and other mammalian cell types (e.g., Gadsby and Nakao, 1989; Bielen et al., 1991; Kinard et al., 1994; Peluffo et al., 2000). Also consistent with this effect being mediated via the external transport sites, the K^+ congeners Cs^+, Rb^+, and Tl^+, all slowed activation of PTX-induced current in side-by-side comparisons with Na^+- or NMG^+-containing external solutions (Fig. 7 C). Notably, in the extreme case of Tl^+ (present as 145 mM $TlNO_3$), 100 nM PTX appeared incapable of activating any current, although 500 nM PTX was able to very slowly ($\tau_{inc} > 2{,}000$ s) elicit the conductance (not depicted). This inhibitory influence cannot be attributed to the NO_3^- ions, as addition of 100 nM PTX in external solution containing principally $NaNO_3$ rapidly activated the conductance, with a

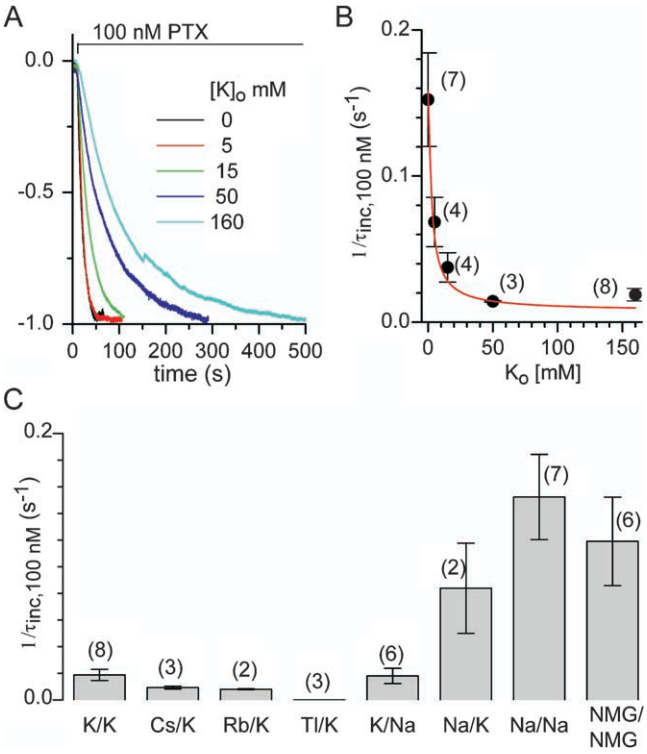

FIGURE 7. Slow activation of I_{PTX} with K^+ external solution is due to K^+ binding at its transport sites. (A) Superimposed records of normalized I_{PTX} activated by 100 nM PTX in outside-out patches (at −20 mV, with 150 mM Na^+ and 5 mM MgATP in the pipette), showing slowing of activation by increasing external [K^+] (with [K^+]+[Na^+] = 160 mM). (B) Mean (±SEM, of n measurements) $1/\tau_{inc}$ for 100 nM PTX plotted against external [K^+]; red line shows Michaelis fit yielding $K_{0.5K} = 2.4 \pm 1.2$ mM, $1/\tau_{inc}(max) = 0.16 \pm 0.03\ s^{-1}$, and $1/\tau_{inc}(min) = 0.007 \pm 0.003\ s^{-1}$. (C) Mean (±SEM, of n measurements) rates of I_{PTX} activation by 100 nM PTX with indicated ionic conditions (external cation/internal cation): K^+/K^+, $0.019 \pm 0.004\ s^{-1}$; Cs^+/K^+, $0.009 \pm 0.001\ s^{-}$; Rb^+/K^+, $0.008 \pm 0.0004\ s^{-1}$; Tl^+/K^+, $0\ s^{-1}$; K^+/Na^+, $0.018 \pm 0.004\ s^{-1}$; Na^+/K^+, $0.084 \pm 0.034\ s^{-1}$; Na^+/Na^+, $0.15 \pm 0.03\ s^{-1}$; NMG^+/NMG^+, $0.12 \pm 0.03\ s^{-1}$.

rate of $1/\tau_{inc} = 0.07 \pm 0.03\ s^{-1}$ ($n = 2$), similar to that in the usual Na-sulfamate solution.

Influence of Nucleotides on PTX–Pump Interactions

One of the differences between the experimental conditions described above with Na^+-containing internal solution, and those with exclusively K^+ in the internal solution, is that only in the former case is it certain that the Na/K pumps would be phosphorylated by the included MgATP. With that in mind, we examined PTX interactions with the Na/K pump in HEK293 cell patches bathed in all-Na^+ solutions, but either with nucleotides omitted or with 2 mM MgAMPPNP in the pipette, for comparison with the data already obtained using 5 mM MgATP. (We took care to allow ≥10 min equilibration with these pipette solutions, interspersed

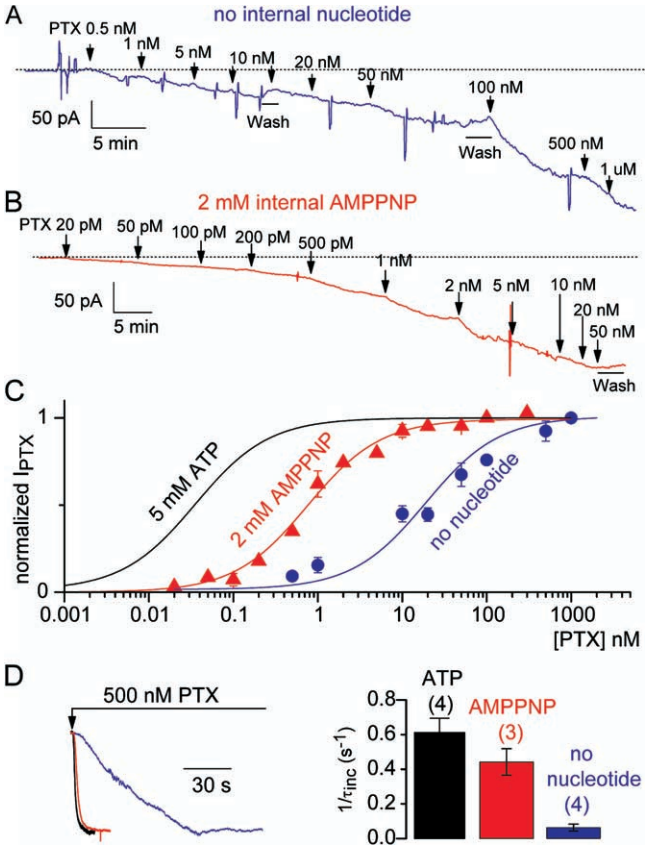

FIGURE 8. PTX apparent affinity is reduced by ATP depletion. (A and B) Activation of I_{PTX} at −20 mV by incremental increases in [PTX] in outside-out HEK293 cell patches with 160 mM external Na^+ and 150 mM internal Na^+ solutions, with either (A) no nucleotide or (B) 2 mM MgAMPPNP in the pipette. The discernible current decay elicited by even brief (100–150-s) wash periods indicates the more rapid unbinding of PTX in these solutions than with MgATP in the pipette (compare with Fig. 4 A, above). (C) Mean estimated steady I_{PTX} amplitude (from exponential fits), normalized to that at 100 nM PTX, was plotted against log [PTX] and fitted with Michaelis functions, which gave $K_{0.5PTX}$ = 19 ± 3 nM for patches with no nucleotides (blue circles, n = 6) and $K_{0.5PTX}$ = 0.76 ± 0.08 nM with MgAMPPNP (red triangles, n = 2); for display, the data with no nucleotides were renormalized to I_{PTX}(max) from the fit. The curve obtained with 5 mM MgATP (Fig. 4 C) is also shown (black line, $K_{0.5PTX}$ = 33 pM) for comparison. (D, left) Normalized records showing rate of I_{PTX} activation by 500 nM PTX in outside-out patches with no nucleotide (blue trace), with 2 mM MgAMPPNP (red trace), or with 5 mM MgATP (black trace) in the internal solution. (Right) Bar graph summarizing $1/\tau_{inc}$: mean rates were 0.61 ± 0.08 s^{-1} with MgATP (black bar; n = 4), 0.44 ± 0.08 s^{-1} with MgAMPPNP (red bar; n = 3), and 0.06 ± 0.02 s^{-1} without nucleotide (blue bar; n = 4).

with frequent exposures to external K^+ solution, to ensure that any initially phosphorylated Na/K pumps would become dephosphorylated.) Upon exposure to increasing concentrations of PTX in the absence of pipette nucleotides, 1 nM PTX activated very little current (Fig. 8 A), in contrast to the almost maximal effect obtained with 1 nM PTX in the presence of 5 mM MgATP (compare Fig. 4, above); in fact, with no nucleotides, maximal current activation required ∼1 μM PTX. Indeed, Michaelis-Menten fits to the mean data in the absence of nucleotides (Fig. 8 C, blue circles) yielded $K_{0.5PTX}$ = 19 ± 3 nM (n = 6), confirming that the apparent affinity for PTX was reduced ∼1,000-fold compared with 5 mM MgATP (Fig. 8 C, black line, $K_{0.5PTX}$ = 33 pM; data from Fig. 4 C, above).

To address whether this reduced affinity might be attributable to lack of phosphorylation, we repeated the measurements with pipette solution containing 2 mM MgAMPPNP (Fig. 8 B), a poorly hydrolyzable MgATP analogue that is essentially incapable of phosphorylating the Na/K pump (ouabain-sensitive Na- and Mg-dependent hydrolysis of AMPPNP is <1% of that of ATP at 20°C; Schuurmans-Stekhoven et al., 1983), but that readily binds to the pump and supports K/K exchange (Simons, 1975). With AMPPNP in the pipette, 1 nM PTX activated a substantial, but still not maximal, current (Fig. 8 B). The dependence on [PTX] of the mean steady-state amplitude of PTX-induced current obtained with 2 mM MgAMPPNP (Fig. 8 C, red triangles) gave $K_{0.5PTX}$ = 0.76 ± 0.07 nM (n = 2). In a single experiment with 2 mM MgADP in the pipette $K_{0.5PTX}$ was 0.33 nM (not depicted), comparable to the value obtained with MgAMPPNP.

The greatly reduced apparent affinity in the absence of nucleotide seems due both to a reduced rate of current activation (Fig. 8 D) and to an increased rate of current decline after withdrawal of the toxin that reflects its unbinding (τ_{dec} = 1,330 ± 260 s, n = 7, estimated from washout periods >400 s; e.g., Artigas and Gadsby, 2003a). This ∼10-fold faster current decay than seen with MgATP in the pipette ($\tau_{dec} > 2 \times 10^4$ s; e.g., Fig. 4 A, above) was similarly found for PTX washout in the presence of MgAMPPNP (τ_{dec} = 2,740 ± 1,090 s, n = 4; estimated as in the absence of nucleotide). Interestingly, however, though current activation by high [PTX] was slowed (∼10-fold, Fig. 8 D) by the absence of nucleotide, it was just as rapid with MgAMPPNP in the pipette as with MgATP.

The clear separation of the three curves in Fig. 8 C (5 mM MgATP, 2 mM MgAMPPNP, and no nucleotides) suggests that the influence of [MgATP] on PTX affinity might be seen over two distinct ranges of nucleotide concentration, the submicromolar range that supports pump phosphorylation (Post et al., 1965) and the submillimolar range that promotes ion deocclusion (Forbush, 1987a). To investigate that possibility, $K_{0.5PTX}$ was determined using cumulative dose-response curves (as in Figs. 4 A, 5 A, and 8, A and B) at each of several concentrations of pipette nucleotide, either MgATP or MgAMPPNP. The summarized data (Fig. 9) confirm that $K_{0.5PTX}$ did indeed show a biphasic dependence on cytoplasmic [MgATP] (filled circles) that could be described empirically as the sum of two Michaelis equa-

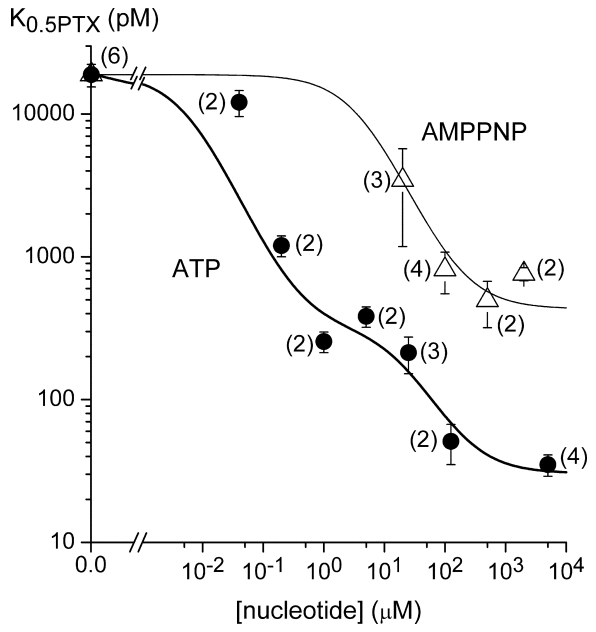

FIGURE 9. Dependence of $K_{0.5PTX}$ on type and concentration of internal nucleotide. Estimates of steady I_{PTX} levels at several [PTX] were determined as in Figs. 4 A and 8, A and B, in outside-out HEK293 cell patches with Na^+ external and internal solutions, but with one of a range of concentrations of MgATP or of MgAMPPNP in the pipette. For each [nucleotide], $K_{0.5PTX}$ was obtained from a Michaelis fit to the data from *n* patches and is shown plotted against [nucleotide] on log–log axes. The $K_{0.5PTX}$ values for 0 μM ≤ [MgATP] ≤ 5 mM (filled circles) are approximated (fitted line) by the sum of two Michaelis components (plus a constant, C) with amplitude and $K_{0.5}$ parameters: A_1 = 18.9 nM, $K_{0.5ATP\text{-}1}$ = 5.5 nM, A_2 = 280 pM, $K_{0.5ATP\text{-}2}$ = 19 μM, and C = 20 pM. The $K_{0.5PTX}$ values for 0 μM ≤ [MgAMPPNP] ≤ 2 mM (open triangles) are described (fitted line) by a single Michaelis function (plus a constant, C) with parameters: A_1 = 18.9 nM, $K_{0.5AMPPNP}$ = 4 μM, and C = 430 pM.

tions (thick fit line) with half-maximal MgATP concentrations reflecting action at high and low apparent affinity sites, $K_{0.5HATP}$ = 6 nM and $K_{0.5LATP}$ = 19 μM, respectively. In contrast, the influence of cytoplasmic [MgAMPPNP] on $K_{0.5PTX}$ (empty triangles) was reasonably approximated by a single Michaelis function (thin fit line) with half-maximal MgAMPPNP concentration, $K_{0.5AMPPNP}$ = 4 μM. This influence of MgAMPPNP was exerted over a comparable concentration range to the lower-affinity effect of MgATP, despite the fact that the minimum $K_{0.5PTX}$ at high [nucleotide] was ~400 pM for MgAMPPNP but was ~20 pM for MgATP.

Interaction between PTX and Cardiotonic Steroids

Previous reports have noted that, in several preparations, preincubation of cells with a cardiotonic steroid, like ouabain, could preclude an increase in membrane permeability when a low concentration of PTX was subsequently applied in the continued presence of the steroid, even though that [PTX] was sufficient to measurably increase permeability when applied alone without any preexposure to the pump inhibitor (e.g., Habermann and Chhatwal, 1982; Ozaki et al., 1984; Wang and Horisberger, 1997). In preliminary outside-out patch, as well as whole-cell, current recordings from HEK293 cells, however, we found that even in the continuous presence of ouabain the PTX-induced conductance could be activated very slowly by concentrations of PTX high enough (100 nM) to promptly activate the conductance in the absence of any ouabain. So, persistent occupancy of the pumps by the cardiotonic steroid (either uninterrupted, or due to repeated rebinding) markedly reduced the apparent affinity for PTX interaction. One mechanism to explain the slowed action we observed for a high concentration of PTX in the presence of ouabain, therefore, is that dissociation of the steroid from the pump might be a prerequisite for activation of the PTX-induced conductance. Because time courses of effects in the simultaneous presence of cardiotonic steroid and PTX are expected to be complex functions of the binding and unbinding rates of both molecules to and from the Na/K pump, we simplified matters by limiting measurements to conditions with these ligands present only one at a time in the external solution.

When outside-out patches from HEK293 cells were exposed to 100 nM PTX at the end of a 5-min preincubation with a saturating concentration (0.5–1 mM) of ouabain, dihydrouabain, or strophathidin, the rates of activation of the PTX-induced conductance were much lower than when the preincubation had been without any cardiotonic steroid (Fig. 10). Moreover, although the PTX solution was devoid of cardiotonic steroid, activation of the conductance was far slower (note logarithmic time scale) after preincubation with ouabain (red trace) than it was after preincubation with strophanthidin (blue trace) or dihydroouabain (green trace). Because ouabain is known to unbind from Na/K pumps more slowly than the other two steroids (e.g., Yoda and Yoda, 1977), these results imply that, after preincubation with cardiotonic steroid, activation of I_{PTX} requires unbinding of the steroid from Na/K pumps.

But, is PTX unable to bind to the cardiotonic steroid–pump complex and so must await steroid unbinding, or can both molecules engage a single Na/K pump at the same time, in which case the apparent affinity for each ligand may be modified by the presence of the other? To address this, we measured the time course of PTX-induced conductance activation in HEK293 cell patches after a 5-min preincubation with 0.5 mM strophanthidin, as in Fig. 10, but using two PTX concentrations, 100 nM (Fig. 11 A, thin trace) and 1 μM PTX (Fig. 11 A, thick trace). The sample records, normalized for kinetic comparison, show that conductance increased more rapidly (~6-fold, Fig. 11 B) with 1 μM than with 100 nM PTX under otherwise identical con-

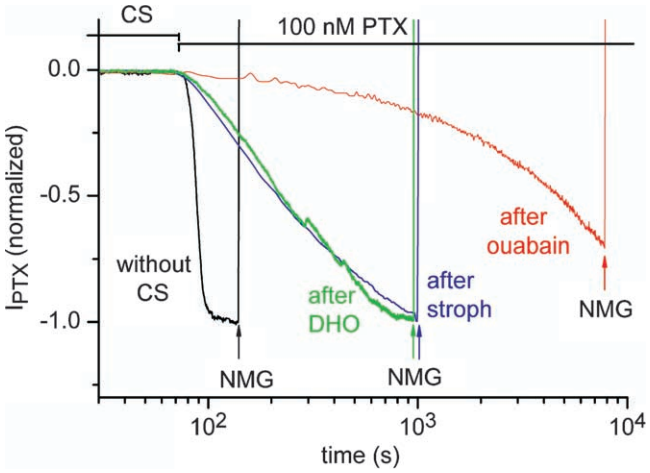

FIGURE 10. Preincubation with a cardiotonic steroid (CS) slows subsequent activation of I_{PTX} by 100 nM PTX after washout of the steroid. Superimposed records of normalized (to the maximum from exponential fits) I_{PTX} at −20 mV in outside-out HEK293 cell patches with Na^+ external and internal solutions and 5 mM internal MgATP; note logarithmic time scale. PTX was applied after 5-min preincubations with 1 mM ouabain (red trace, τ_{inc} = 7250 s), or 0.5 mM strophanthidin (blue trace, τ_{inc} = 240 s), or 1 mM dihydroouabain (DHO, green trace, τ_{inc} = 257 s), or with no CS (black trace, τ_{inc} = 6 s).

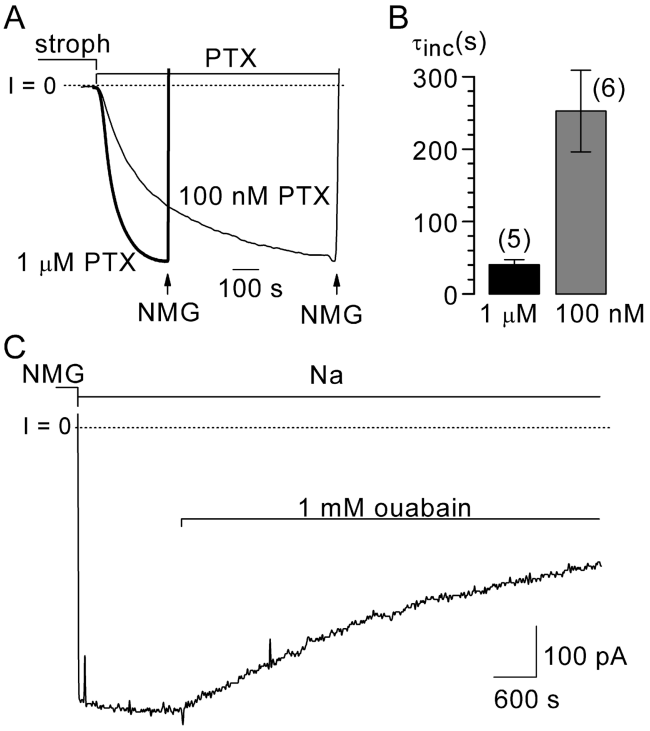

FIGURE 11. PTX and ouabain can simultaneously occupy the same Na/K pump in HEK293 cells. (A) Superimposed representative normalized records of I_{PTX} activation at −20 mV in outside-out HEK293 cell patches with Na^+ external and internal solutions and 5 mM internal MgATP, after 5-min preincubation with 0.5 mM strophanthidin. I_{PTX} increased more slowly with 100 nM PTX (thin trace) than with 1 μM PTX (thick trace). (B) Bar graph summarizing several (*n*) measurements: mean τ_{inc} was 256 ± 53 s with 100 nM PTX and 41 ± 7 s with 1 μM PTX. (C) Continuation of red trace from Fig. 10, after activation of I_{PTX} in Na^+ solution and 1.5 min of PTX washout in NMG^+ solution; current did not decay for ~20 min in Na^+ solution until 1 mM ouabain was added.

ditions. However, with no steroid preincubation, conductance activation was faster still in these solutions, and was complete within 10–20 s for 100 nM (e.g., Fig. 10) and within 2 s for 1 μM (compare 500 nM, Fig. 4 B) PTX. The far slower conductance increases, both with 100 nM and with 1 μM PTX, after preincubation to form the cardiotonic steroid–pump complex, confirm that dissociation of that complex rate limits the increase in conductance. But the more rapid conductance increase elicited by 1 μM than by 100 nM PTX indicates that binding of PTX accelerates dissociation of strophanthidin from its complex with the Na/K pump, and this could occur only if PTX and strophanthidin can simultaneously interact with the same Na/K pump.

The implied reduced affinity for strophanthidin when the Na/K pump is occupied by PTX means that, because of constraints imposed by microscopic reversibility, the apparent affinity for PTX ought to be similarly reduced when the Na/K pump is occupied by strophanthidin. The record in Fig. 11 C shows that after maximal activation of conductance by 100 nM PTX, the current decayed negligibly slowly during ~20 min of toxin washout (compare Fig. 4 A, above), but decayed more rapidly upon exposure to 1 mM ouabain; the same result was obtained with 1 mM dihydroouabain or 0.5 mM strophathidin (not depicted). Because subsequent withdrawal of ouabain (or strophanthidin) did not restore inward current unless PTX was applied again (not depicted), the steroid must have accelerated unbinding of PTX rather than merely diminishing PTX-induced conductance (e.g., by closing PTX-opened pump channels; see Artigas and Gadsby, 2003a). Following the above reasoning, this result indicates that cardiotonic steroids must be able to bind to PTX-modified Na/K pumps. In addition, the slow speed of this action of 1 mM ouabain (τ = 7700 s; Fig. 11 C), a concentration that abolishes Na/K-pump function in seconds (e.g., Fig. 12), further demonstrates the reduced affinity for cardiotonic steroids of a PTX-modified Na/K pump.

Our conclusion, that the time course of conductance activation by PTX after preincubation with cardiotonic steroid (Fig. 11, A and B) reflects accelerated steroid unbinding due to binding of PTX, implies that dissociation of the steroid in the absence of PTX should be measurably slower. The time course of Na/K pump current recovery upon washout of cardiotonic steroid provides a reasonable estimate of steroid unbinding rate in the absence of PTX. Because the small amplitude of Na/K

pump current in HEK293 cells (Kocksämper et al., 1997) made accurate measurements difficult, we used guinea-pig ventricular myocytes instead (e.g., Gadsby and Nakao, 1989), and exploited the rapid reversibility of dihydroouabain (e.g., Gao et al., 1995). During strong activation of outward Na/K pump current under whole-cell current recording with 50 mM pipette Na^+ and 5 mM MgATP, and 30 mM extracellular Cs^+ (as K^+ congener), exposure to 1 mM dihydroouabain caused a sudden inward current shift (Fig. 12 A) due to inhibition of the entire population of myocyte Na/K pumps. Dissociation of dihydroouabain after its washout then slowly restored outward pump current ($t_{0.5}$ = 53 ± 7 s, n = 14, Fig. 12 D). Reapplication of dihydroouabain again abolished Na/K pump current and, once inhibition was complete, a patch of membrane was excised in the outside-out configuration with all pumps still inhibited. Upon exposure to 1 μM PTX, concomitant with removal of dihydroouabain (Fig. 12 B), the PTX-induced conductance was activated in the subpopulation of pumps in the patch more rapidly ($t_{0.5}$ = 18 ± 2 s, n = 8) than the pump current had recovered in that myocyte's entire pump population after washout of dihydroouabain alone. In agreement with the results in HEK293 cells (Fig. 10), PTX-induced conductance activation in myocyte patches was much faster in the absence of cardiotonic steroid ($t_{0.5}$ = 2.5 s, Fig. 12, C and D; but with otherwise identical solutions) than after the preincubation with dihydroouabain (Fig. 12, B and D), confirming that the latter slower time course reflects dissociation of bound steroid (in the presence of PTX). The even slower time course of pump current reactivation after washout of dihydroouabain alone (Fig. 12, A and D) demonstrates that PTX speeds dihydroouabain dissociation from the pump–steroid complex (as similarly concluded above for strophanthidin; Fig. 11, A and B), and hence that the two ligands must be able to interact with the same Na/K pump at the same time.

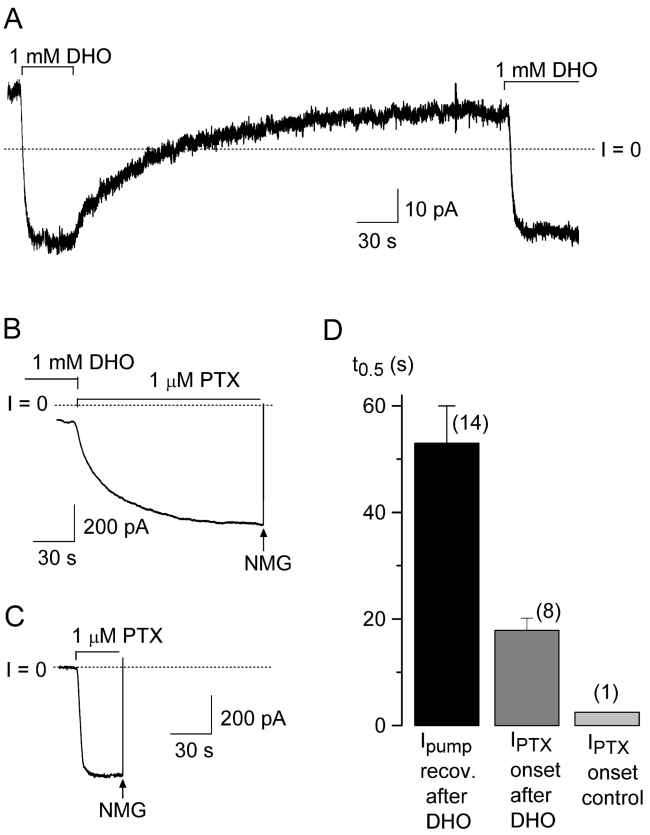

FIGURE 12. PTX accelerates unbinding of cardiotonic steroids in ventricular myocytes. (A) Whole-cell current at −2 mV with 30 mM external Cs^+ and 50 mM internal Na^+; 1 mM DHO abolished outward Na/K pump current, I_{pump}, which recovered with $t_{0.5}$ = 60 s after DHO washout. (B) During second exposure to DHO, an outside-out patch was excised from the myocyte in A, and 1 μM PTX was applied as DHO was withdrawn, activating I_{PTX} with $t_{0.5}$ = 20 s. (C) Rapid activation of I_{PTX} with same solutions as in A and B, but with no DHO preincubation; patch from different myocyte. (D) Bar graph summarizing $t_{0.5}$ values from experiments as in A–C.

DISCUSSION

To better understand PTX interactions with the Na/K pump, we used excised outside-out patches for optimal control of conditions and we systematically varied the nucleotides in the pipette and the ions at the two membrane surfaces. We found that the apparent affinity for PTX could be reproducibly varied over several orders of magnitude, and was highest when Na/K pumps were exposed to K^+-free, Na^+-containing external and internal solutions and to high cytoplasmic [MgATP]. We found that PTX and a cardiotonic steroid can simultaneously occupy the same Na/K pump, but that each weakens the binding of the other. We found that the narrowest part of the permeation pathway through the PTX-induced channel must be ∼7.5 Å wide. We next discuss the implications of these results.

Influence of Nucleotides on PTX–Na/K Pump Interactions

MgATP is known to influence Na/K pump function both in the submicromolar range, at which concentrations it phosphorylates the pump in the presence of cytoplasmic-side Na^+ (Post et al., 1965), as well as in the submillimolar range over which it promotes deocclusion and release of K^+ toward the cytoplasmic side (Forbush, 1987a). Only the latter low-affinity action can be mimicked by poorly hydrolyzable nucleotides like AMP-PNP or ADP (Simons, 1975; Kaplan and Kenney, 1982). We have previously shown that application of millimolar MgATP, MgAMPPNP, or MgADP instantaneously increased (∼6-fold) the open probability of PTX-bound pump channels in excised inside out patches with saturating [PTX] in the pipette (Artigas and Gadsby, 2003a), indicating that low-affinity nucleotide interaction persists in PTX-modified Na/K pumps. However,

several of our findings indicate that high-affinity MgATP action, hence at the phosphorylation site, can also influence the PTX–Na/K pump complex. Thus, despite the above-mentioned similar actions of MgATP, MgAMP-PNP, and MgADP on the P_o of PTX-induced channels, $K_{0.5PTX}$, a measure of the apparent affinity for PTX action, was at least 10-fold smaller in patches equilibrated with Na solutions containing 5 mM MgATP than in patches equilibrated (≥10 min) with pipette solutions containing 2 mM MgAMPPNP or 2 mM MgADP (Fig. 8 C), suggesting that prior phosphorylation of Na/K pumps (expected with MgATP, but not MgAMPPNP or MgADP) influences their interaction with PTX. This conclusion is further supported by the finding that equilibration with pipette solutions containing different [MgATP] influenced $K_{0.5PTX}$ over both submicromolar and submillimolar concentration ranges, whereas varying [MgAMPPNP] affected $K_{0.5PTX}$ only within the submillimolar concentration range (Fig. 9). Moreover, because we found that the decay of PTX-induced current upon PTX washout (in K-containing external solution), which reflects PTX unbinding (Artigas and Gadsby, 2003a), occurred rapidly when the pipette solution contained either no nucleotides or 2 mM MgAMPPNP, but was severalfold slower when pipettes contained 1 μM or 5 mM MgATP (Artigas and Gadsby, 2003b), we conclude not only that phosphorylation of Na/K pumps strengthens their interaction with PTX, but also that PTX-bound Na/K pumps exposed to MgATP likely remain phosphorylated for minutes.

To further interpret the large variations in $K_{0.5PTX}$ we observed with different pipette solutions, we consider a simplified scheme (Scheme I) that treats the Na/K pump, once it has bound PTX, as a channel that is either closed (C) or open (O), ignoring the gating complexities evident in preliminary single-channel dwell-time histograms that likely arise from the presence of two separate channel gates (Artigas and Gadsby, 2003a). As no channel activity is seen in the absence of PTX, toxin must first bind to the pump enzyme (E) before it can elicit the open-channel conformation; for simplicity, we assume that toxin also unbinds from the closed-channel state; this assumption is consistent with the observations that PTX unbinding rates (e.g., Figs. 4 and 5) are much lower than opening and closing rates of PTX-bound channels (Fig. 3; cf. Artigas and Gadsby, 2003a). This simplest scheme thus comprises three states:

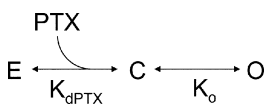

SCHEME I

At steady state, distributions among these conformations are determined both by the equilibrium dissociation constant, K_{dPTX} ($=k_{off}/k_{on}$, the ratio of dissociation and association rate constants), for PTX binding to state E, and by the equilibrium constant, K_o, between closed- and open-channel states of the PTX-bound pump, K_o ($=k_o/k_c$, the ratio of the rate constants for channel opening and channel closing). Accordingly, the apparent dissociation constant for palytoxin ($K_{0.5PTX}$) will depend both on the open probability of a PTX-bound pump channel ($P_o = k_o/(k_o + k_c) = K_o/(K_o + 1)$) and on K_{dPTX}, and will approach the latter only if P_o is very small (i.e., if K_o is very small):

$$K_{0.5PTX} = K_{dPTX}/(1 + K_o) = (1 - P_o)K_{dPTX}. \quad (1)$$

This relation allows estimation of K_{dPTX} from the $K_{0.5PTX}$ values determined in Figs. 8 C and 9 under conditions for which P_o is also known. From single-channel current recordings in outside-out patches from cardiac myocytes, with Na-containing solutions, P_o was ∼0.9 (K_o ∼9) for PTX-induced channels in the presence of 5 mM MgATP, but was reduced to $P_o \leq 0.2$ in the absence of nucleotide (Artigas and Gadsby, 2003a). The rapid six-fold increase in PTX-induced current in larger inside-out patches upon suddenly switching from ATP-free to 5-mM MgATP-containing solution (Artigas and Gadsby, 2003a) suggests that a reasonable estimate for P_o is ∼0.15 (∼0.9/6; i.e., K_o ∼0.18) in the absence of nucleotide. Thus, for 5 mM MgATP, $K_{0.5PTX}$ ∼30 pM = $0.1K_{dPTX}$, yielding K_{dPTX} ∼300 pM. In the absence of nucleotide, $K_{0.5PTX}$ averaged ∼19 nM = $0.85K_{dPTX}$, which yields K_{dPTX} ∼22 nM. Because addition of 1 μM MgATP only slightly increased PTX-induced current in inside-out patches (by <10% of the maximal increase seen with 5 mM MgATP; Artigas and Gadsby, 2003a), the channel P_o in 1 μM MgATP may be assumed comparable to that in the absence of nucleotide, and so the $K_{0.5PTX}$ of ∼250 pM in 1 μM MgATP (Fig. 9) corresponds to a K_{dPTX} ∼300 pM. Like MgATP, 2 mM MgAMPPNP increased macroscopic PTX-induced current ∼6-fold in inside-out myocyte patches (Artigas and Gadsby, 2003a), indicating that P_o in high [MgAMPPNP] is close to that in high [MgATP], and so the mean $K_{0.5PTX}$ value of ∼760 pM (Fig. 8) implies that K_{dPTX} is ∼8 nM in MgAMPPNP.

These values allow parsing of the influences on K_{dPTX} of pump phosphorylation and of low-affinity nucleotide binding, if we make the simplifying assumptions that 1 μM MgATP supports phosphorylation but negligible occupancy of the low-affinity sites, that 5 mM MgATP supports both phosphorylation and low-affinity binding, and that 2 mM MgAMPPNP supports low-affinity binding but no phosphorylation. Within these assumptions, phosphorylation of the pump alone appears responsible for the ∼70-fold smaller K_{dPTX} seen with 1 μM MgATP (∼300 pM) than with no nucleotides (∼22 nM); this stimulatory influence of phosphorylation (at the cytoplasmic side of the pump) on

PTX binding (at the extracellular side) seemed little altered by occupancy of low-affinity nucleotide sites (at the cytoplasmic side), viz. K_{dPTX} of ~300 pM with 5 mM MgATP vs. ~8 nM with 2 mM MgAMPPNP, a ~30-fold enhancement of PTX affinity. In contrast, the affinity for PTX seemed only modestly enhanced by low-affinity nucleotide binding, regardless of whether the pumps were phosphorylated (K_{dPTX} ~300 pM with either 1 μM or 5 mM MgATP) or unphosphorylated (K_{dPTX} ~22 nM without nucleotides vs. ~8 nM with 2 mM MgAMPPNP). Similarly, in work on red blood cell membranes, ATP, and to a lesser extent ADP, was shown to promote PTX-mediated cation flux (Chhatwal et al., 1983), to enhance ^{125}I-PTX binding (Böttinger et al., 1986), and to promote opening of channels in inside-out patches when PTX was in the pipette (Kim et al., 1995).

As already mentioned, this enhanced affinity of PTX for phosphorylated pumps seems at least partly attributable to slowed dissociation. This is evident whether PTX unbinding is monitored simply from current decay upon PTX withdrawal in external Na^+ (~10-fold slower with 5 mM MgATP in the pipette than with 2 mM MgAMPPNP or no nucleotides; e.g., Figs. 4 and 8, above) or assessed by residual current in external Na^+ after brief exposures to external K^+ (severalfold slower with 1 μM or 5 mM MgATP than with 2 mM MgAMPPNP or no nucleotides; Artigas and Gadsby, 2003b).

PTX Alters the Na/K Pump's Phosphorylation Status

Further implications of the large influence on PTX affinity of phosphorylation by 1 μM MgATP become clear when states corresponding to those in Scheme I are linked by explicit phosphorylation reactions (justified by the above conclusion that PTX-bound pumps appear to remain phosphorylated). In Scheme II, the subscript P identifies phosphorylated states (E_P, C_P, O_P), and the K_{pho} are lumped equilibrium constants that incorporate all steps involved in pump phosphorylation and dephosphorylation.

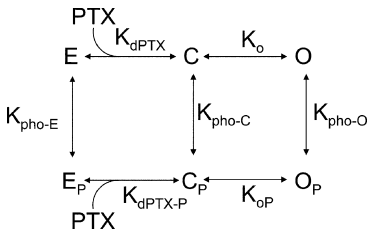

SCHEME II

Because the P_o of PTX-bound pump channels is comparable with 0 or 1 μM MgATP (hence K_o K_{oP}; Artigas and Gadsby, 2003a), microscopic reversibility dictates that the equilibrium constants that describe phosphorylation of open and closed channel states, K_{pho-O} and K_{pho-C}, must also be similar. By the same token, the very different K_{dPTX} values of phosphorylated and unphosphorylated pumps (K_{dPTX-P} ~300 pM vs. K_{dPTX} ~22 nM; see above) means that the equilibrium constant for phosphorylation of unmodified pumps (K_{pho-E}) must differ strongly from those of toxin-bound pumps (K_{pho-C}, and hence also K_{pho-O}), via:

$$K_{dPTX-P} \cdot K_{pho-C} = K_{dPTX} \cdot K_{pho-E}.$$

Our numbers yield $K_{pho-C} = 70K_{pho-E}$, which indicates a substantial shift toward the phosphorylated state in the PTX–pump complex. The lumped phosphorylation–dephosphorylation reaction comprises Na^+- and ATP-binding steps, phosphoryl transfer, and dephosphorylation, all steps that have been well characterized in unmodified pumps, though not after modification by PTX (but see Tosteson et al., 2003). In either case, the high (150 mM) pipette [Na^+], and the presence of ATP but nominal absence of ADP ought to render the phosphorylation steps kinetically irreversible. A reasonable explanation, then, for the ~70-fold enhanced phosphorylation constant of PTX-bound pumps, is that dephosphorylation of the pump is somehow impaired once PTX is bound. The presence of 160 mM external Na^+ is likely to drive dephosphorylation of the normal, unmodified pumps via a Na,Na-ATPase cycle, in which occlusion of 2 Na^+ (in place of the normal 2 K^+) is associated with loss of phosphate. If dephosphorylation similarly requires ion occlusion in PTX-bound pumps, then the apparent propensity of PTX to interfere with closure of the external gate to the cation-binding cavity (Artigas and Gadsby, 2003a,b) offers a possible mechanism for how PTX may impair both occlusion and dephosphorylation. It is not clear how this inference of enhanced pump phosphorylation by MgATP in the presence of PTX relates to a recent conclusion that PTX impaired phosphorylation of purified Na,K-ATPase from MgATP, but enhanced phosphorylation from P_i (Tosteson et al., 2003).

Nucleotide Interactions with their Low-affinity Binding Site on the Na/K Pump

Analysis of low-affinity nucleotide interactions requires that states appropriate for 1 μM MgATP and those expected at saturating (i.e., 5 mM) MgATP be linked by nucleotide binding reactions (Scheme III); an analogous scheme can be used for a comparison of observations without nucleotide and with 2 mM MgAMPPNP:

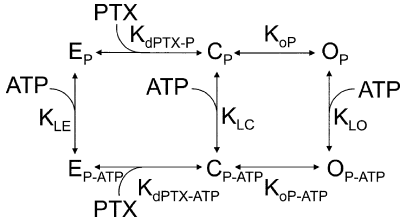

SCHEME III

As already noted, K_{dPTX} for phosphorylated pumps ($K_{dPTX\text{-}P}$ in Scheme III) was ~300 pM at 1 μM MgATP and was apparently unaffected by low-affinity ATP binding, being also ~300 pM at 5 mM MgATP ($K_{dPTX\text{-}ATP}$ in Scheme III). In unphosphorylated pumps, too, K_{dPTX} was only little affected by low-affinity nucleotide binding, being ~22 nM without nucleotides and ~8 nM with 2 mM MgAMPPNP. For both these cases, then, microscopic reversibility (applied to Scheme III) requires that the equilibrium dissociation constants for low-affinity nucleotide binding to the unmodified pump, K_{LE}, and to the closed state of the PTX-bound pump channel, K_{LC}, be roughly the same. However, channel open probability (and hence K_o) is greatly increased upon nucleotide binding to the low affinity site (Artigas and Gadsby, 2003a), yielding values of $K_{oP} \approx 0.18$, and $K_{oP\text{-}ATP} \approx 9$. Because microscopic reversibility forces:

$$K_{LC} \cdot K_{oP} = K_{LO} \cdot K_{oP\text{-}ATP},$$

we conclude that $K_{LC} \approx 50\ K_{LO}$, where K_{LO} is the dissociation constant for low-affinity binding of MgATP to the open-channel state. In other words, MgATP binds with 50-fold higher affinity to the open state of the PTX-bound pump channel than to its closed state (or to the unmodified pump). But can we estimate absolute values?

By considering only the PTX-bound states in Scheme III, we can express the open probability, i.e., the steady-state fractional occupancy of states O_P and $O_{P\text{-}ATP}$, as a function of [ATP]:

$$P_o = ([ATP] + K_{LO})/\{(K_{LO}(1 + K_{oP})/K_{oP}) + ([ATP](1 + K_{oP\text{-}ATP})/K_{oP\text{-}ATP})\}.$$

If occupancy of state $O_{P\text{-}ATP}$ is assumed negligible at 1 μM ATP, and of state O_P is negligible at 5 mM ATP, this can be written as

$$P_o = ([ATP] + K_{LO})/\{(K_{LO}/P_{omin}) + ([ATP]/P_{omax})\},$$

where P_{omin} is the open probability at 0 (or 1 μM) ATP, and P_{omax} is the P_o at 5 mM ATP. Because PTX dissociates so slowly, the variation of PTX-induced macroscopic current (reflecting the change in P_o, ΔP_o) with changes of [ATP] bathing inside-out patches, could be approximated by the Michaelis function:

$$\Delta P_o = (P_{omax} - P_{omin})[ATP]/(K_{0.5ATP} + [ATP]),$$

where $K_{0.5ATP} = K_{LO}P_{omax}/P_{omin}$.

The fit gave ~20 μM for $K_{0.5ATP}$ (Artigas and Gadsby, 2003a), and since P_{omax}/P_{omin} is ~6, the dissociation constant for low-affinity ATP binding to the open-channel state, K_{LO}, ~3 μM, which in turn means that K_{LC}, for the closed state, is ~150 μM. Because the latter should also apply to the unmodified pump (as $K_{LC} \approx K_{LE}$, above), it is of interest that comparable values have been obtained for the apparent affinity with which ATP accelerates Na,K-ATPase activity (Post et al., 1972; Moczydlowski and Fortes, 1981) or ouabain-sensitive K/K exchange (Simons, 1974), or accelerates deocclusion of K^+ toward the pump's cytoplasmic surface (Forbush, 1987a,b), or activates pump current amplitude (Friedrich et al., 1996). Insofar as the rate-limiting step in the entire Na,K-ATPase cycle is K^+ deocclusion, ATP may be expected to exert its effect in all these instances by binding at the low-affinity site. Correspondingly, we interpret the ATP-induced increment in the P_o of PTX-induced channels as reflecting opening of the cytoplasmic-side gate in response to low-affinity binding of the nucleotide to the PTX–pump complex.

Because cytoplasmic K^+ deocclusion normally follows dephosphorylation in unmodified Na/K pumps, it is not surprising that similar considerations apply to AMPPNP (which cannot support phosphorylation). Thus, we found that 2 mM MgAMPPNP essentially mimics the effects of low-affinity ATP binding in that it little altered K_{dPTX} (see above) but markedly increased, ~6-fold, the P_o of PTX-bound pump channels (Artigas and Gadsby, 2003a).

Influence of External K^+ or Cardiotonic Steroids on PTX–Na/K Pump Interactions

A comparably detailed analysis of the reductions in apparent PTX affinity we observed (all in the presence of 5-mM pipette MgATP) on replacing external and/or internal Na^+ by K^+, or upon exposure to cardiotonic steroids, is presently not possible because we know little about the P_o of PTX-bound pump channels under those conditions. External K^+ ions are able to shut PTX-bound pump channels, and hence lower P_o, in the absence of nucleotides (Artigas and Gadsby, 2003a), and also in the presence of MgAMPPNP (Artigas and Gadsby, 2003b), but we lack evidence for K^+-induced changes in P_o in the presence of high [MgATP]. Nevertheless, because 5 mM MgATP was always present in the conditions under consideration, if we use all-Na^+ solutions as our reference point (P_o ~0.9), Eq. 1 indicates that even a reduction in P_o to zero could account for no more than a 10-fold increase in $K_{0.5PTX}$. The observed ~100-fold increases in $K_{0.5PTX}$ on replacing external Na^+ by K^+, regardless of whether the principal internal cation was Na^+ (~30 pM increased to ~3 nM; Figs. 4 C and 6 D) or K^+ (~300 pM increased to ~30 nM; Figs. 6 B and 5 C), therefore imply that external K^+ ions act on the Na/K pump to reduce its true affinity for PTX. This interpretation is supported by the parallel finding that external K^+ also acted to accelerate (~30-fold, with either internal Na^+ or K^+; e.g., Figs. 4 A

and 5 A) the slow deactivation of PTX-induced current after PTX washout that likely reflects PTX unbinding. These results confirm earlier demonstrations of antagonism by external K^+ of PTX action (Ahnert-Hilger et al., 1982) or of ^{125}I-PTX binding (Böttinger et al., 1986), and of relief of PTX-mediated inhibition of ATPase activity by increasing $[K^+]$ (Ishida et al., 1983).

We have not measured the P_o of PTX-bound pump channels in the presence of cardiotonic steroids. But, our finding that higher [PTX] speeds the (still slowed) opening of channels in pumps initially complexed with a cardiotonic steroid (Fig. 11, A and B), apparently by speeding dissociation of that complex, demonstrates not only that PTX and steroid can occupy the same Na/K pump molecule (as does the steroid-induced speeding of PTX dissociation; Fig. 11 C), but also that such a PTX-bound pump channel does not open until the steroid has unbound. In other words, the bound steroid must sustain a closed conformation of the PTX-bound pump channel, which in turn implies that binding of the steroid would lower P_o of pump channels opened by PTX. Though that fall in P_o would contribute to an increase in $K_{0.5PTX}$ (though <10-fold), the marked steroid-mediated reduction we observed in apparent affinity for PTX action (e.g., Figs. 10 and 11, as previously reported: Chhatwal et al., 1983; Habermann, 1989) and the acceleration of PTX unbinding (Fig. 11 C) both indicate that, when also bound to the Na/K pump, the steroids directly increase K_{dPTX}.

In unmodified Na/K pumps, replacement of external Na^+ by K^+ promotes K^+-ion occlusion in the dephosphorylated conformation $E_2(K_2)$ (e.g., Beaugé and Glynn, 1979), whereas, in all-Na^+ solutions with MgATP, addition of cardiotonic steroids promotes Na^+-ion occlusion in the phosphorylated conformation $E_2P(Na_2)$ (e.g., Stürmer and Apell, 1992). The salient common factor is closure of an external gate, which can also explain the common tendencies of these two maneuvers both to lower the P_o of PTX-bound pump channels and to destabilize the PTX–Na/K pump complex.

Which Na/K Pump Conformation Binds PTX with Highest Affinity?

Previous authors have favored E_1 (e.g., Scheiner-Bobis and Schneider, 1997) or E_2 (e.g., Wang and Horisberger, 1997) or both (Habermann, 1989) conformations of the Na/K pump as the state(s) to which PTX prefers to bind (for review see Tosteson, 2000). Given that an unmodified Na/K pump can support a maximal uphill Na^+-ion efflux of $\leq 5 \times 10^2$ ions s^{-1}, whereas the channel in a PTX-bound Na/K pump can pass a dissipative Na^+-ion influx of $\geq$0.8 pA (Fig. 3 C; i.e., $\geq 5 \times 10^6$ ions s^{-1}), the probability that such an open-channel conformation can exist in an unmodified pump must be extremely small, $<10^{-4}$. In other words, the Na/K pump conformation stabilized by PTX is not likely to be any of the states visited in the familiar Post-Albers kinetic scheme for ion transport by the Na/K pump. Indeed, our results show that PTX binds with highest affinity to phosphorylated Na/K pumps exposed to K^+-free, high $[Na^+]$ external and internal solutions with MgATP. In these conditions, the pumps may be expected to largely populate E_2P conformations in the steady state. As mentioned, the subsequent slow current decline on PTX withdrawal, reflecting slow dissociation of PTX, implies that the pumps remained phosphorylated as long as PTX was bound, and hence that the ATPase cycle was stalled before the dephosphorylation step. But high concentrations of PTX could also open pump channels during exposure to Na^+-free, high $[K^+]$ internal and external solutions, in which, despite the presence of 5 mM internal MgATP, the predominant steady-state conformations are expected to be nonphosphorylated E_1 states (equally true for all Na^+ solutions with no, or nonhydrolyzable, nucleotide), and ATPase cycling should also be precluded. In terms of the alternating-gate scheme of pump-mediated Na/K transport, in which access to binding sites is controlled by an extracellular-side gate in E_2 conformations and by a cytoplasmic-side gate in E_1 conformations, PTX-induced channel states with both gates open must be hybrids with features of both E_1 and E_2 conformations. Despite the absence of ATPase cycles (Ishida et al., 1983), however, PTX-bound pumps are not restricted to a single conformational state, as ligand-mediated gating events persist that appear to resemble normal partial reactions of the pump associated with occlusion and deocclusion of transported cations (Artigas and Gadsby, 2003a). Because PTX-bound pump channels in physiologically relevant solutions, with high $[Na^+]$ and with millimolar [MgATP], display a P_o of $\sim$0.9, it appears that PTX has evolved to bind most tightly to, and hence to most effectively stabilize, the conformation that is most lethal to animal cells.

Simultaneous Na/K Pump Occupancy by a Cardiotonic Steroid and PTX

While earlier work pointed to some form of competition between PTX and cardiotonic steroids (for review see Habermann, 1989; Tosteson, 2000), the results presented here establish that both of these large compounds can simultaneously interact with the same Na/K pump. The clearest demonstration is that each can accelerate the unbinding from the Na/K pump of the other. Because both PTX (Muramatsu et al., 1984) and cardiotonic steroids (e.g., Forbush et al., 1978) are believed to exert their action by binding to the external surface of the pump, we must conclude that a single

Na/K pump can simultaneously accommodate at least some portion of a ~2.7-kD PTX molecule and some part of a ~0.5-kD cardiotonic steroid molecule. Although a combination of mutagenesis (e.g., Price and Lingrel, 1988; Canessa et al., 1993; Palasis et al., 1996; Koenderink et al., 2000) and structure-function (e.g., Middleton et al., 2000; Sweadner and Donnet, 2001; Ball et al., 2003) analyses are helping to identify the docking sites for cardiotonic steroids, there is as yet no information about where or how the large, extended-chain PTX molecule interacts with the exterior of the Na/K pump.

Implications of Permeation Data

The single-channel conductance of ~7 pS found here for PTX-induced channels in native Na/K pumps of guinea-pig ventricular myocytes during exposure to all-Na^+ solutions fits with the 7–10 pS values reported previously for various preparations (e.g., Ikeda et al., 1988; Muramatsu et al., 1988; Rettinger and Schwarz, 1994; Kim et al., 1995; Hirsh and Wu, 1997; Wang and Horisberger, 1997). Use of the outside-out patch configuration in the present work allowed unambiguous identification of PTX-induced pump channel currents as those elicited exclusively upon addition of the toxin. A novel finding was the unequivocal demonstration that N-methyl-D-glucamine, with an average diameter of ~7.3 Å, could pass through the open channel, whereas the ≥8-Å diameter tetrapropylammonium could not. This prompts further questions. First, if the pore is so wide, why is the single-channel conductance for Na^+ only ~7 pS? A possible explanation is that more than one ion can occupy the pore at a time, and that ions interact within the pore. Measurements of tracer flux-ratio exponents should help evaluate this possibility (Rakowski et al., 2003).

Second, is this wide pore part of the normal ion pathway negotiated by the transported Na^+ and/or K^+ ions? If it is, then the observed throughput rate of $\geq 5 \times 10^6$ Na^+ ions s^{-1} provides a lower estimate for the dissociation rate of the tightest Na^+-binding sites within the pore; assuming a diffusion-limited binding rate of 10^9 M^{-1} s^{-1} at those sites, their dissociation constant could be no smaller than 5 mM. As K^+ ions are conducted even more rapidly than Na^+, they must bind even more loosely within the pore. These considerations indicate that, if the pore is part of the normal ion translocation pathway, the Na^+- and/or K^+-ion binding sites with submillimolar apparent affinity in the unmodified Na/K pump (e.g., Bühler and Apell, 1995; Schneeberger and Apell, 2001) must be characteristic of conformations in which one or other of the pump's two gates is closed. Initial evidence that the pore of PTX-induced channels comprises at least some segment of the ion-translocation pathway comes from cysteine-scanning mutagenesis studies (Guennoun and Horisberger, 2000, 2002). PTX was found to render accessible to small water-soluble sulfhydryl-specific reagents cysteine residues introduced at positions in the fifth and sixth transmembrane helices that are believed to help coordinate the transported ions, on the basis of site-specific mutagenesis experiments (e.g., Nielsen et al., 1998; Pedersen et al., 1998) and of homology modelling (Ogawa and Toyoshima, 2002; Rakowski and Sagar, 2003) using the crystal structures of the related SERCA pump (Toyoshima et al., 2000; Toyoshima and Nomura, 2002). Additional evidence that the pore of PTX-bound pump channels usurps the normal ion translocation path is provided by our demonstration that the P_o of those channels can be modulated by ligands of the Na/K pump in a manner consistent with their known action to favor occlusion or deocclusion of the transported ions (Artigas and Gadsby, 2003a,b). Interestingly, the SERCA pump structures appear to incorporate relatively wide access channels. Thus, a cavity was observed in the 8-Å resolution E2-decavanadate SERCA pump structure (Zhang et al., 1998), consistent with a water-filled access channel to the ion binding sites from the lumen (equivalent to the extracellular side in the Na/K pump). Also, the high-resolution E2-thapsigargin structure (Toyoshima and Nomura, 2002) contained a water-accessible channel, lined with negatively charged residues, leading toward the binding sites from the cytoplasmic side. These access channel-like structures in SERCA pumps are in accord with our data that suggest the presence of a ~7.5-Å wide ion pathway in a PTX-modified Na/K pump. If the PTX-induced pore does indeed comprise at least some part of the binding pocket(s) occupied by occluded Na^+ and/or K^+ ions during their transport by the unmodified pump, then the improved understanding of PTX's interaction with the Na/K pump afforded by the present work should now allow use of PTX to help reveal the locations, structures, and mechanisms of the Na/K pump's gates that alternately occlude and deocclude the transported ions.

We thank Claudia Basso and Miguel Holmgren for help with preliminary experiments and for much useful discussion.

This work was supported by NIH HL-36783.

Michael L. Jennings served as guest editor.

Submitted: 20 October 2003
Accepted: 5 February 2004

REFERENCES

Artigas, P., and D.C. Gadsby. 2003a. Na^+/K^+ ligands modulate gating of palytoxin-induced ion channels. *Proc. Natl. Acad. Sci. USA.* 100:501–505.

Artigas, P., and D.C. Gadsby. 2003b. Ion occlusion/deocclusion partial reactions in individual palytoxin-modified Na/K pumps. *Ann. NY Acad. Sci.* 986:116–126.

Ahnert-Hilger, G., G.S. Chhatwal, H.J. Hessler, and E. Habermann. 1982. Changes in erythrocyte permeability due to palytoxin as compared to amphotericin B. *Biochim. Biophys. Acta.* 688:486–494.

Ball, W.J., Jr., C.D. Farr, S. Paula, S.M. Keenan, R.K. Delisle, and W.J. Welsh. 2003. Three-dimensional structure-activity relationship modeling of digoxin inhibition and docking to Na^+,K^+-ATPase. *Ann. NY Acad. Sci.* 986:296–297.

Beaugé, L.A., and I.M. Glynn. 1979. Occlusion of k ions in the unphosphorylated sodium pump. *Nature.* 280:510–512.

Bielen, F.V., H.G. Glitsch, and F. Verdonck. 1991. Dependence of Na^+ pump current on external monovalent cations and membrane potential in rabbit cardiac Purkinje cells. *J. Physiol.* 442: 169–189.

Böttinger, H., L. Béress, and E. Habermann. 1986. Involvement of (Na^+K)-ATPase in binding and actions of palytoxin on human erythrocytes. *Biochim. Biophys. Acta.* 861:165–176.

Bühler, R., and H.J. Apell. 1995. Sequential potassium binding at the extracellular side of the Na,K-pump. *J. Membr. Biol.* 145:165–173.

Canessa, C.M., J.D. Horisberger, and B.C. Rossier. 1993. Mutation of a tyrosine in the H3-H4 ectodomain of Na,K-ATPase alpha subunit confers ouabain resistance. *J. Biol. Chem.* 268:17722–17726.

Chhatwal, G.S., H.J. Hessler, and E. Habermann. 1983. The action of palytoxin on erythrocytes and resealed ghosts. Formation of small, nonselective pores linked with Na^+, K^+-ATPase. *Naunyn Schmiedebergs Arch. Pharmacol.* 323:261–268.

Dwyer, T.M., D.J. Adams, and B. Hille. 1980. The permeability of the endplate channel to organic cations in frog muscle. *J. Gen. Physiol.* 75:469–492.

Forbush, B., III, J.H. Kaplan, and J.F. Hoffman. 1978. Characterization of a new photoaffinity derivative of ouabain: labeling of the large polypeptide and of a proteolipid component of the Na, K-ATPase. *Biochemistry.* 17:3667–3676.

Forbush, B., III. 1987a. Rapid release of ^{42}K and ^{86}Rb from an occluded state of the Na,K-pump in the presence of ATP or ADP. *J. Biol. Chem.* 262:11104–11115.

Forbush, B., III. 1987b. Rapid release of ^{42}K or ^{86}Rb from two distinct transport sites on the Na,K-pump in the presence of Pi or vanadate. *J. Biol. Chem.* 262:11116–11127.

Friedrich, T., E. Bamberg, and G. Nagel. 1996. Na,K-ATPase pump currents in giant excised patches activated by an ATP concentration jump. *Biophys. J.* 71:2486–2500.

Gadsby, D.C., and M. Nakao. 1989. Steady-state current-voltage relationship of the Na/K pump in guinea pigventricular myocytes. *J. Gen. Physiol.* 94:511–537.

Gao, J., R.T. Mathias, I.S. Cohen, and G.J. Baldo. 1995. Two functionally different Na/K pumps in cardiac ventricular myocytes. *J. Gen. Physiol.* 106:995–1030.

Guennoun, S., and J.-D. Horisberger. 2000. Structure of the 5th transmembrane segment of the Na,K-ATPase alpha subunit: a cysteine-scanning mutagenesis study. *FEBS Lett.* 482:144–148.

Guennoun, S., and J.-D. Horisberger. 2002. Cysteine-scanning mutagenesis study of the sixth transmembrane segment of the Na,K-ATPase alpha subunit. *FEBS Lett.* 513:277–281.

Habermann, E., and G.S. Chhatwal. 1982. Ouabain inhibits the increase due to palytoxin of cation permeability of erythrocytes. *Naunyn Schmiedebergs Arch. Pharmacol.* 319:101–107.

Habermann, E. 1989. Palytoxin acts through Na^+ K^+ ATPase. *Toxicon.* 27:1171–1187.

Hamill, O.P., A. Marty, E. Neher, B. Sakmann, and F.J. Sigworth. 1981. Improved patch-clamp-techniques for high-resolution current recording from cells and cell-free membrane patches. *Pflugers Arch.* 391:85–100.

Hille, B. 1992. Ionic Channels in Excitable Membranes. Sinauer, Sunderland, MA.

Hirsh, J.K., and C.H. Wu. 1997. Palytoxin-induced single-channel currents from the sodium pump synthesized by in vitro expression. *Toxicon.* 35:169–176.

Ikeda, M., K. Mitani, and K. Ito. 1988. Palytoxin induces a nonselective cation channel in single ventricular cells of rat. *Naunyn-Schmiedeberg's Arch Pharmacol.* 337:591–593.

Ishida, Y., K. Takagi, M. Takahashi, N. Satake, and S. Shibata. 1983. Palytoxin isolated from marine coelenterates. The inhibitory action on (Na^+,K^+)-ATPase. *J. Biol. Chem.* 258:7900–7902.

Kang, T.M., V.S. Markin, and D.W. Hilgemann. 2003. Ion fluxes in giant excised cardiac membrane patches detected and quantified with ion-selective microelectrodes. *J. Gen. Physiol.* 121:325–347.

Kaplan, J.H., and L.J. Kenney. 1982. ADP supports ouabain-sensitive K-K exchange in human red blood cells. *Ann. NY Acad. Sci.* 402:292–295.

Kim, S.Y., K.A. Marx and C.H. Wu. 1995. Involvement of Na,K-ATPase in the induction of ion channels by palytoxin. *Naunyn-Schmiedeberg's Arch Pharmacol.* 351:542–554.

Kinard, T.A., X.Y. Liu, S. Liu, and J.R. Stimers. 1994. Effect of Na_{pip} on K_o activation of the Na-K pump in adult rat cardiac myocytes. *Am. J. Physiol.* 266:C37–C41.

Kocksämper, J., G. Gisselmann, and H.G. Glitch. 1997. Comparison of ouabain-sensitive and -insensitive Na/K pumps in HEK 293 cells. *Biochim. Biophys. Acta.* 1325:197–208.

Koenderink, J.B., H.P. Hermsen, H.G. Swarts, P.H. Willems, and J.J. De Pont. 2000. High-affinity ouabain binding by a chimeric gastric H^+,K^+-ATPase containing transmembrane hairpins M3-M4 and M5-M6 of the alpha 1-subunit of rat Na^+,K^+-ATPase. *Proc. Natl. Acad. Sci. USA.* 97:11209–11214.

Middleton, D.A., S. Rankin, M. Esmann, and A. Watts. 2000. Structural insights into the binding of cardiac glycosides to the digitalis receptor revealed by solid-state NMR. *Proc. Natl. Acad. Sci. USA.* 97:13602–13607.

Moczydlowski, E.G., and P.A. Fortes. 1981. Inhibition of sodium and potassium adenosine triphosphatase by 2′,3′-O-(2,4,6-trinitrocyclohexadienylidene) adenine nucleotides. Implications for the structure and mechanism of the Na:K pump. *J. Biol. Chem.* 256:2357–2366.

Moore, R.E., and P.J. Scheuer. 1971. Palytoxin: a new marine toxin from coelenterate. *Science.* 172:495–498.

Muramatsu, I., D. Uemura, M. Fujiwara, and T. Narahashi. 1984. Characteristics of palytoxin-induced depolarization in squid giant axons. *J. Pharmacol. Exp. Ther.* 231:488–494.

Muramatsu, I., M. Nishio, S. Kigoshi, and D. Uemura. 1988. Single ionic channels induced by palytoxin in guinea pig ventricular myocytes. *Br. J. Pharmacol.* 93:811–816.

Nielsen, J.M., P.A. Pedersen, S.J. Karlish, and P.L. Jorgensen. 1998. Importance of intramembrane carboxylic acids for occlusion of K+ ions at equilibrium in renal Na,K-ATPase. *Biochemistry.* 37: 1961–1968.

Ogawa, H., and C. Toyoshima. 2002. Homology modeling of the cation binding sites of Na^+K^+-ATPase. *Proc. Natl. Acad. Sci. USA.* 99:15977–15982.

Ozaki, H., H. Nagase, and N. Urawa. 1984. Sugar moiety of cardiac glycosides is essential for the inhibitory action on the palytoxin-induced K^+ release from red blood cells. *FEBS Lett.* 173:196–199.

Palasis, M., T.A. Kuntzweiler, J.M. Arguello, and J.B. Lingrel. 1996. Ouabain interactions with the H5-H6 hairpin of the Na,K-ATPase reveal a possible inhibition mechanism via the cation binding domain. *J. Biol. Chem.* 271:14176–14182.

Pedersen, P.A., J.M. Nielsen, J.H. Rasmussen, and P.L. Jorgensen. 1998. Contribution to Tl+, K+, and Na+ binding of Asn776,

Ser775, Thr774, Thr772, and Tyr771 in cytoplasmic part of fifth transmembrane segment in alpha-subunit of renal Na,K-ATPase. *Biochemistry.* 37:17818–17827.

Peluffo, R.D., J.M. Arguello, and J.R. Berlin. 2000. The role of Na,K-ATPase alpha subunit serine 775 and glutamate 779 in determining the extracellular K+ and membrane potential-dependent properties of the Na,K-pump. *J. Gen. Physiol.* 116:47–59.

Post, R.L., A.K. Sen, and A.S. Rosenthal. 1965. A phosporylated intermediate in adenosine triphosphate-dependent sodium and pottassium transport across kidney membranes. *J. Biol. Chem.* 240:1437–1445.

Post, R.L., C. Hegyvary, and S. Kume. 1972. Activation by adenosine triphosphate in the phosphorylation kinetics of sodium and potassium ion transport adenosine triphosphatase. *J. Biol. Chem.* 247:6530–6540.

Price, E.M., and J.B. Lingrel. 1988. Structure-function relationships in the sodium-potassium ATPaseα subunit: site-directed mutagenesis of glutamine-111 to arginine and asparagine-122 to aspartic acid generates a ouabain-resistant enzyme. *Biochemistry.* 27: 8400–8408.

Rakowski, R.F., and S. Sagar. 2003. Found: Na^+ and K^+ binding sites of the sodium pump. *News Physiol. Sci.* 18:164–168.

Rakowski, R.F., P. Artigas, M. Holmgren, D.C. Gadsby, and P. DeWeer. 2003. Na ion occupancy of the channels opened by palytoxin. *Biophys. J.* 84:P320a.

Redondo, J., B. Fiedler, and G. Scheiner-Bobis. 1996. Palytoxin-induced Na^+ influx into yeast cells expressing the mammalian sodium pump is due to the formation of a channel within the enzyme. *Mol. Pharmacol.* 49:49–57.

Rettinger, J., and W. Schwarz. 1994. Ion selective channels in K562 cells: a patch-clamp analysis. *J. Basic Clin. Physiol. Pharmacol.* 5:27–44.

Robinson, R.A., and R.H. Stokes. 1965. Electrolyte Solutions. Butterworths, London. 571 pp.

Rouzaire-Dubois, B., and J.M. Dubois. 1990. Characterization of palytoxin-induced channels in mouse neuroblastoma cells. *Toxicon.* 28:1147–1158.

Scheiner-Bobis, G., D. Meyer zu Heringdorf, M. Christ, and E. Habermann. 1994. Palytoxin induces K^+ efflux from yeast cells expressing the mammalian sodium pump. *Mol. Pharmacol.* 45:1132–1136.

Scheiner-Bobis, G., and H. Schneider. 1997. Palytoxin-induced channel formation within the Na^+/K^+-ATPase does not require a catalytically active enzyme. *Eur. J. Biochem.* 248:717–723.

Schneeberger, A., and H.J. Apell. 2001. Ion selectivity of the cytoplasmic binding sites of the Na,K-ATPase: II. Competition of various cations. *J. Membr. Biol.* 179:263–273.

Schuurmans-Stekhoven, F.M., H.G. Swarts, J.J. De Pont, and S.L. Bonting. 1983. Hydrolysis of adenylyl imidodiphosphate in the presence of $Na^+ + Mg^{2+}$ by $(Na^+ + K^+)$-activated ATPase. *Biochim. Biophys. Acta.* 736:73–78.

Simons, T.J.B. 1974. Potassium-potassium exchange catalyzed by the sodium pump in human red cells. *J. Physiol.* 237:123–155.

Simons, T.J.B. 1975. The interaction of ATP-analogues possessing a blocked gamma-phosphate group with the sodium pump in human red cells. *J. Physiol.* 244:731–739.

Stürmer, W., and H.-J. Apell. 1992. Fluorescence study on cardiac glycoside binding to the Na,K-pump. Ouabain binding is associated with movement of electrical charge. *FEBS Lett.* 300:1–4.

Sweadner, K., and C. Donnet. 2001. Structural similarities of Na,K-ATPase and SERCA, the Ca^{2+}-ATPase of the sarcoplasmic reticulum. *Biochem. J.* 356:685–704.

Taylor, T.J., G.W. Parker, A.B. Fajer, and K.A. Mereish. 1991. Nonspecific binding of palytoxin to plastic surfaces. *Toxico. Lett.* 57: 291–296.

Tosteson, M.T., J.A. Halperin, Y. Kishi, and D.C. Tosteson. 1991. Palytoxin induces an increase in the cation conductance of red cells. *J. Gen. Physiol.* 98:969–985.

Tosteson, M.T. 2000. Mechanism of action, pharmacology and toxicology. *In* Seafood and Freshwater Toxins Pharmacology, Physiology, and Detection. L.M. Botana, editor. Marcel Dekker, New York-Basel. 549–566.

Tosteson, M.T., J. Thomas, J. Arnadottir, and D.C. Tosteson. 2003. Effects of palytoxin on cation occlusion and phosphorylation of the (Na^+,K^+)-ATPase. *J. Membr. Biol.* 192:181–189.

Toyoshima, C., M. Nakasako, H. Nomura, and H. Ogawa. 2000. Crystal structure of the calcium pump of sarcoplasmic reticulum at 2.6 Å resolution. *Nature.* 405:647–655.

Toyoshima, C., and H. Nomura. 2002. Structural changes in the calcium pump accompanying the dissociation ofcalcium. *Nature.* 418:605–611.

Villarroel, A., N. Burnashev, and B. Sakmann. 1995. Dimensions of the narrow portion of a recombinant NMDA receptor channel. *Biophys. J.* 68:866–875.

Wang, X., and J.-D. Horisberger. 1997. Palytoxin effect through interaction with the Na,K-ATPase in *Xenopus* oocytes. *FEBS Lett.* 409:391–395.

Weidmann, S. 1977. Effect of palytoxin on the electrical activity of dog and rabbit heart. *Experientia.* 33:1487–1489.

Yoda, S., and A. Yoda. 1977. Association and dissociation rate constants of the complexes between various cardiac aglycones and sodium- and potassium-dependent adenosine triphosphatase formed in the presence of magnesium and phosphate. *Mol. Pharmacol.* 13:352–361.

Zhang, P., C. Toyoshima, K. Yonekura, N.M. Green, and D.L. Stokes. 1998. Structure of the calcium pump from sarcoplasmic reticulum at 8-A resolution. *Nature.* 392:835–839.